Available online at www.sciencedirect.com

SCIENCE DIRECT®

Lithos 79 (2005) 1–24

LITHOS

www.elsevier.com/locate/lithos

An overview of adakite, tonalite–trondhjemite–granodiorite (TTG), and sanukitoid: relationships and some implications for crustal evolution

H. Martin[a,*], R.H. Smithies[b], R. Rapp[c], J.-F. Moyen[d], D. Champion[e]

[a]*Laboratoire Magmas et Volcans; OPGC-Université Blaise Pascal–CNRS; 5, rue Kessler; 63038 Clermont-Ferrand Cedex, France*
[b]*Geological Survey of Western Australia, 100 Plain Street, East Perth, WA 6004, Australia*
[c]*Geodynamics Research Centre; Ehime University; 2-5 Bunkyo-cho, Matsuyama; 790-8577, Japan*
[d]*Department of Geology, University of Stellenbosch. Private Bag X 01, 7602 Matieland, South Africa*
[e]*Geosciences Australia, GPO Box 378, Canberra, ACT 2601, Australia*

Received 16 October 2003; accepted 2 September 2004

Abstract

Examination of an extensive adakite geochemical database identifies two distinct compositional groups. One consists of high-SiO_2 adakites (HSA) which is considered to represent subducted basaltic slab-melts that have reacted with peridotite during ascent through mantle wedge. The second group consists of low-SiO_2 adakites (LSA) which we interpret to have formed by melting of a peridotitic mantle wedge whose composition has been modified by reaction with felsic slab-melts.

The chemical composition of less differentiated (primitive) Archaean tonalite–trondhjemite–granodiorite (TTG) magmas evolved from 4.0 to 2.5 Ga. Mg# (molecular $Mg/(Mg+Fe^{2+})$, Ni, and Cr contents increased over this period of time and we interpret these changes in terms of changes in the degree to which the TTG magmas interacted with mantle peridotite. Over the same period, concentrations of ($CaO+Na_2O$) and Sr also increased, as the amount of plagioclase, residual from basalt melting, decreased in response to increased pressures at the site of slab-melting. In the Early Archaean, it appears that these interactions were very rare or absent thus leading to the conclusion that subduction was typically flat and lacked the development of a mantle wedge. In contrast, the relatively lower heat production by ~2.5 Ga meant that slab-melting occurred at greater depth, where plagioclase was no longer stable, and where the development of a thick mantle wedge ensured interaction between the slab-melts and mantle peridotite.

Close compositional similarities between HSA and Late Archaean TTG (T<~3.0 Ga) strongly suggest a petrogenetic analogy. However, an analogy between the older Archaean TTG and HSA is not complete because evidence for mantle wedge interaction is missing in most Early Archaean TTGs.

Late Archaean sanukitoids and the compositionally similar Closepet-type granites have compositions significantly different from TTG of all ages. However, they show some affinity with LSA which could be considered as their possible analogue. These magmas are all thought to result from melting of a mantle peridotite whose composition has been modified by reaction with slab-melts.

* Corresponding author. Tel.: +33 04 73 34 67 40; fax: +33 04 73 34 67 44.
E-mail address: h.martin@opgc.univ-bpclermont.fr (H. Martin).

0024-4937/$ - see front matter © 2004 Published by Elsevier B.V.
doi:10.1016/j.lithos.2004.04.048

We propose that all these magmas are directly linked to slab-melting. Archaean TTG and HSA represent slab-melts that have interacted with peridotite to varying extent, whereas sanukitoids, Closepet-type granites, and LSA correspond to melts of peridotite previously metasomatised by slab-melt. The changes observed from Early Archaean TTG to Late Archaean TTG and to sanukitoids reflect change in both the nature and efficiency of interaction between slab-melt and mantle wedge peridotite. Comparisons between all of these rocks suggest that ancient styles of subduction that have operated since at least ~3.3 Ga persist in a limited way today. The secular changes in the degree and style of these interactions is a direct consequence of the cooling of Earth that modified the thermal and dynamic parameters at the subducted slab–mantle wedge interface.

Keywords: Adakite; TTG; Sanukitoid; Crustal evolution; Archaean

1. Introduction

Although most modern subduction zone magmas are thought to reflect partial melting of metasomatised mantle wedge peridotite, recent studies have shown that subduction zone magmas can also be produced by fusion of subducted oceanic crust basalts. These typically sodic and felsic 'slab-melts' were termed adakites by Defant and Drummond (1990) in reference to the work done by Kay (1978) on magnesian andesites from Adak Island in the Aleutians. Slab-melting had already been proposed elsewhere to account for similar lavas (Condie and Swenson, 1973; Lopez-Escobar et al., 1977; Kay, 1978). The interpretation of adakites as slab-melts is supported by experimental work on water-saturated or dehydration melting of amphibolites (Beard and Lofgren, 1989, 1991; Rapp et al., 1991; Rushmer, 1991; Winther and Newton, 1991; Wolf and Wyllie, 1991; Sen and Dunn, 1994a) as well as by observational evidence of adakitic glass inclusions in xenoliths within subduction related lavas (Schiano et al., 1995), and adakitic veins in ophiolites (Sorensen and Barton, 1987; Sorensen, 1988; Sorensen and Grossman, 1989; Bebout and Barton, 1993).

Slightly before these works on adakite, studies on Archaean sodic rocks of tonalite, trondhjemite, and granodiorite composition had already suggested a connection between sodic, felsic magmatism, and melting of basaltic crust at pressures high enough to stabilise garnet (eclogite- or garnet-bearing amphibolite; Barker and Arth, 1976; Hunter et al., 1978; Barker et al., 1979; Tarney et al., 1979, 1982; Condie, 1981; Jahn et al., 1981; Martin et al., 1983; Sheraton and Black, 1983). These tonalites, trondhjemites, and granodiorites were collectively termed the 'TTG suite' by Jahn et al. (1981) and have become one of the defining features of Archaean terranes. Condie (1981) was among the first to apply the concepts of modern plate tectonics to the origin of TTG when he proposed that the basaltic source for these rocks might have been subducted oceanic crust. Martin (1986, 1988) proposed that modern lavas from the Austral Volcanic Zone in Chile (not then known as adakites) may represent modern equivalents of Archaean TTG. The view that adakite and TTG represent petrogenetic analogues has since become widely accepted and was reiterated and expanded by Martin (1999).

A significantly rarer, but also widespread, feature of Archaean terranes is a distinctive series of high-Mg dioritic, tonalitic, and granodioritic rocks first identified by Shirey and Hanson (1984) and referred to Archaean sanukitoids. Now described from most Late Archaean terranes (Shirey and Hanson, 1984; Stern, 1989; Stern and Hanson, 1991; Smithies and Champion, 1999a), these rocks, as well as the closely related high-Mg and high-K granites called "Closepet-type" granites (Moyen et al., 2001, 2003a; Martin and Moyen, 2003), are interpreted to represent melting of a mantle wedge peridotite previously metasomatised through interaction with slab-melts. Adakites, TTGs, and sanukitoids are all interpreted to have a direct or indirect petrogenetic link to partial melting of basaltic crust, and, if not explicitly, (Martin, 1986, 1988, 1999) then implicitly (Smithies and Champion, 2000; Smithies et al., 2003) with some form of subduction. They form the components of a distinct class of felsic igneous rocks. However, the precise petrogenetic relationship between these components is not always straightforward. For example, recent studies have shown that the analogy between adakite and TTG is not always simple and unequivocal, nor even appro-

priately applied to TTGs of all ages (Smithies, 2000; Smithies and Champion, 2001; Martin and Moyen, 2002; Rapp, 2003; Smithies et al., 2003). Complicating, or perhaps even causing, such issues is the fact that terms such as 'TTG' have, on the one hand, assumed a distinct petrogenetic significance but have, on the other hand, become a convenient 'bin' for any Archaean plutonic rock with a vaguely sodic chemistry. At the same time, there has been a growing recognition that the pool of rocks now grouped as adakites, or as adakitic, in fact includes at least two major, compositionally distinct groups with significantly different petrogeneses. It may also encompass sodic magmas thought to derive from magmatically thickened mafic arc-crust (Atherton and Petford, 1993), or delaminated mafic crust in apparently nonsubduction-related setting (Xu et al., 2002). The recognition that both 'adakite' and 'TTG' have become terms that individually encompass a complex range of compositions clearly complicates any attempt to draw petrogenetic analogies between the two groups. This overview synthesizes current data on modern rocks classified as 'adakites', concentrating on identifying and characterizing specific subgroups and interpreting their petrogenesis. Against these rocks, we compare the data for Archaean TTG and sanukitoids and investigate the extent and nature of any petrogenetic links.

2. Adakites

2.1. Definition

As originally defined (Defant and Drummond, 1990; Maury et al., 1996; Martin, 1999), adakites form suites of intermediate to felsic rocks whose compositions range from hornblende–andesite to dacite and rhyolite; basaltic members are lacking. In these lavas, phenocrysts are mainly zoned plagioclase, hornblende, and biotite; orthopyroxene and clinopyroxene phenocrysts are known only in mafic andesites from the Aleutians and Mexico (Kay, 1978; Rogers et al., 1985; Calmus et al., 2003). Accessory phases are apatite, zircon, sphene, and titanomagnetite. The rocks have SiO_2>56 wt.%, high Na_2O contents (3.5 wt.%≤ Na_2O≤7.5 wt %), and correlated low K_2O/Na_2O (~0.42). Their Fe_2O_3+MgO+MnO+TiO_2 contents are moderately high (~7 wt.%), with high Mg# (~0.51) and high Ni and Cr contents (24 and 36 ppm, respectively). Defant and Drummond (1990) also reported typically high Sr contents (>400 ppm), with extreme concentrations reaching 3000 ppm. Rare earth element (REE) patterns are strongly fractionated ($(La/Yb)_N$>10) with typically low heavy REE (HREE) contents (Yb≤1.8 ppm, Y≤18 ppm). Amongst the defining geochemical characteristics of adakites are their HREE, Y, and Sr contents, and two widely used discriminant diagrams are $(La/Yb)_N$ vs. Yb_N (Martin, 1987, 1999) (where *N* indicates chondrite normalization), and Sr/Y vs. Y (Defant and Drummond, 1990).

Using a database comprising >340 analyses of 'adakites' classified within the criterion presented above, Martin and Moyen (2003) showed that there are two main compositional groups, which they defined based on their silica content as high-SiO_2 adakites (HSA; SiO_2>60 wt.%) and low-SiO_2 adakites (LSA; SiO_2<60 wt.%). A similar grouping has been independently proposed by Champion and Smithies (2003b). High-SiO_2 adakites include rocks from all the volcanoes of the Austral Volcanic zone of the Andes, excepted the Cook volcano (Stern and Kilian, 1996). They also include El Valle and La Yeguada volcanoes (Panama; Defant et al., 1991, 1992), Mt. St. Helens (USA; Smith and Leeman, 1987), Kalimantan (Borneo; Prouteau et al., 1996), Leyte, Mindanao, and Zamboanga (Philippines; Sajona et al., 1996, 1997), Mezcla (Mexico; Gonzalez-Partida et al., in press), Nevado Cayambe, Pinchincha, Antisana, and Fuya-Fuya (Ecuador; Bourdon et al., 2002; Samaniego et al., 2002, in press), and Sambe and Daisen (Japan; Morris, 1995).

Low-SiO_2 adakites include rocks variably referred to either as high-Mg andesite or as adakite. These have been found from the Cook volcano in the Austral Volcanic zone (Stern and Kilian, 1996), volcanoes from Baja California (Rogers et al., 1985; Calmus et al., 2003), Adak and Kormandosky (Aleutians; Kay, 1978; Yogodzinski et al., 1995), El Baru (Panama; Defant et al., 1992), Zamboanga (Philippines; Sajona et al., 1996), Cono de la Virgen (Ecuador; Samaniego et al., in press), and from Cerro Pampa (Argentina; Mahlburg Kay et al., 1993). These adakites differ from HSA mineralogically primarily in that they may contain pyroxene phenocrysts. Apart from a higher silica content, HSA also have lower MgO (0.5 to 4

wt.%), $CaO+Na_2O$ (<11 wt.%) and Sr (<1100 ppm), compared to LSA (MgO=4–9 wt.%; $CaO+Na_2O$ >10 wt.%; Sr >1000 ppm; Table 1 and Fig. 1). Fig. 2 is a primitive mantle normalized multi-element diagram, which compares LSA and HSA. It shows that (1) LSA have higher LREE concentrations than HSA; (2) LSA display an important positive Sr anomaly that is either slight or absent in HSA; and that (3) LSA are relatively Rb-poor. It must be noted that extreme Sr concentrations are only found in the LSA group. On a plot of (Sr/Y) vs. Y (Fig. 1C), the two groups follow parallel trends with LSA having higher Sr/Y ratios for a given Y concentration. Other significant differences can be seen in the K/Rb ratios and Nb concentrations of the respective groups as well as in Cr/Ni vs. TiO_2 trends (Fig. 1); these are discussed below. Two diagrams that combine these parameters effectively discriminate between the two groups; they are a K/Rb vs. SiO_2/MgO plot, where HSA and LSA form almost perpendicular trends, and a Sr—K/Rb–(SiO_2/MgO)*100 triangular plot (Fig. 3).

2.2. Discussion of main characteristics

2.2.1. Comparison with experimental data

Several experimental studies have involved melting of basalts and amphibolites under various pH_2O conditions below 10 kbar (Holloway and Burnham, 1972; Helz, 1976; Beard and Lofgren, 1989, 1991; Rushmer, 1991). Garnet was not stable in these experiments and the resulting melts were tonalitic in composition, without any trondhjemitic affinity nor HREE impoverishment.

Vapour-absent higher-pressure experiments on metabasalts as well as on modern and Archaean amphibolites (Rapp et al., 1991; Rapp and Watson, 1995; 900–1150 °C; 8–32 kbar), Winther and Newton, 1991; 750–1100 °C; 5–30 kbar), Wolf and Wyllie, 1994; 750–1000 °C; 10 kbar), Sen and Dunn, 1994a; 850–1150 °C; 15–20 kbar), and Zamora, 2000; 1000–1100 °C; 15 kbar)), produced adakitic melts for 10–40% fusion. Residual assemblages comprised plagioclase+amphibole±orthopyroxene±ilmenite at low pressure (8 kbar), garnet+amphibole±plagioclase ±clinopyroxene±ilmenite at 16 kbar, and garnet+clinopyroxene±rutile at higher pressure. Depending upon temperature, garnet becomes stable between about 10 and 12 kbar. The REE contents of the experimental glasses show strongly fractionated adakite-like patterns associated with low HREE contents only where garnet is a stable residual phase (Rapp et al., 1991; Sen and Dunn, 1994b; Wolf and Wyllie, 1994; Rapp and Watson, 1995; Zamora, 2000). The presence of residual hornblende and/or Fe–Ti oxides (rutile, ilmenite) in all experiments most often produces negative Ti–Nb–Ta anomalies like those observed in adakites.

These experimental results are consistent with observations from subducted oceanic basalts from Catalina Island (California; Sorensen and Barton, 1987; Sorensen, 1988; Sorensen and Grossman, 1989; Bebout and Barton, 1993). These metabasalts, now transformed into garnet bearing amphibolites and eclogites, contain migmatitic veins with adakite compositions, interpreted as partial melts formed at 650–750 °C and at 9 to 11 Kbar.

Fig. 4 is a plot of MgO vs. SiO_2, which compares adakite with liquids obtained by experimental melting of basalts or amphibolites. At a given silica content, adakite has higher MgO concentrations than experimental melts. The difference remains small for HSA but it is pronounced in LSA. Several authors (Maury et al., 1996; Stern and Kilian, 1996; Rapp et al., 1999; Smithies, 2000; Prouteau et al., 2001) have interpreted the higher MgO (and also Ni and Cr) contents and Mg# as due to interaction between basalt melt and peridotite. As adakites are almost invariably related to subduction zones those authors further proposed that adakites are subducted-slab-melts whose composition has been modified during their ascent through the mantle wedge, by interaction with mantle peridotite. Rapp et al. (1999) showed that, during ascent through the mantle wedge, slab-melt assimilates peridotite, and that this later undergoes metasomatic reactions involving orthopyroxene and garnet. This process can significantly modify SiO_2, MgO, Ni, and Cr contents, without changing the slab-melt signature as recorded by other trace elements (e.g., REE, Sr, and Y).

Schiano et al. (1995) studied glassy inclusions in olivine crystals from ultramafic mantle xenoliths in lavas from the Batan Islands (Philippines). These inclusions are adakitic in composition, with fractionated REE patterns (average $(La/Yb)_N$=48) associated with low-Yb_N (3.3) and low-Y (5.9 ppm), as well as moderately high Sr (552 ppm) and Sr/Y (93). These inclusions provide direct evidence for interaction

Table 1
Average composition and standard deviation (S.D.) for LSA (Kay, 1978; Rogers et al., 1985; Defant et al., 1991, 1992; Mahlburg Kay et al., 1993; Yogodazinski et al., 1995; Sajona et al., 1996, 1997; Stern and Kilian, 1996; Calmus et al., 2003), HSA (Smith and Leeman, 1987; Defant et al., 1991,1992; Morris, 1995; Sajona, 1995; Prouteau et al., 1996; Stern and Kilian, 1996; Bourdon et al., 2002; Samaniego et al., 2002, 2004; Gonzalez-Partida et al., in press), TTG (Martin, 1994; Martin and Moyen, 2002), Sanukitoids (Shirey and Hanson, 1984, 1986; Querré, 1985; Balakrishnan and Rajamani, 1987; Stern and Hanson, 1991; Krogstad et al., 1995; Smithies and Champion, 1999a; Stevenson et al., 1999; Moyen et al., 2003a), and Closepet-type granites (Jahn et al., 1988; Barton et al., 1992; Jayananda et al., 1995; Frost et al., 1998; Moyen et al., 2001, 2003b)

	LSA (n=77)		HAS (n=267)		TTG>3.5 Ga (n=108)		3 Ga<TTG<3.5 Ga (n=320)		TTG<3 Ga (n=666)		Sanukitoid<62% SiO_2 (n=31)		Closepet<62% SiO_2 (n=43)		Experimental melts (n=27)		Pristine melt
	Average	S.D.	Average	S.D.	Average	S.D.	Average	S.D.	Average	S.D.	Average	S.D.	Average	S.D.	Average	S.D.	
wt.%																	
SiO_2	56.25	3.4	64.80	2.5	69.59	3.1	69.65	3.5	68.36	3.8	58.76	2.9	56.39	3.5	68.94	3.82	66.00
Al_2O_3	15.69	1.1	16.64	0.9	15.29	0.9	15.35	1.3	15.52	1.1	15.80	0.9	15.79	1.4	17.70	1.97	18.00
Fe_2O_3*	6.47	1.5	4.75	1.0	3.26	1.2	3.07	1.6	3.27	1.6	5.87	1.5	7.34	1.7	2.42	1.22	3.63
MnO	0.09	0.02	0.08	0.02	0.04	0.03	0.06	0.05	0.05	0.05	0.09	0.02	0.13	0.08	0.05	0.04	0.04
MgO	5.15	1.5	2.18	0.7	1.00	0.5	1.07	0.6	1.36	0.9	3.90	1.3	3.38	1.9	0.84	0.44	1.03
CaO	7.69	1.0	4.63	0.8	3.03	0.9	2.96	1.2	3.23	1.1	5.57	1.5	5.45	1.4	2.06	0.99	4.43
Na_2O	4.11	0.5	4.19	0.4	4.60	0.5	4.64	0.8	4.70	0.8	4.42	0.7	3.94	0.8	4.92	1.45	5.83
K_2O	2.37	0.8	1.97	0.5	2.04	0.8	1.74	0.7	2.00	0.8	2.78	0.8	3.17	0.8	2.53	1.75	0.51
TiO_2	1.49	0.7	0.56	0.1	0.39	0.3	0.36	0.2	0.38	0.2	0.74	0.3	1.20	0.5	0.78	0.39	0.61
P_2O_5	0.66	0.3	0.20	0.2	0.13	0.09	0.14	0.09	0.15	0.10	0.39	0.1	0.72	0.3			
ppm																	
Rb	19	17	52	21	79	39	59	29	67	51	65	22	93	37	98	48	
Ba	1087	499	721	286	449	323	523	327	847	555	1543	563	1441	653	651	285	
Nb	11	4	6	2	8	7	6	4	7	5	10	8	18	7	11.4	2.4	
Sr	2051	537	565	150	360	116	429	178	541	252	1170	638	978	350	333	169	245
Zr	188	68	108	41	166	64	155	76	154	131	184	129	323	109	196	37	65
Y	13	3	10	3	12	9	14	19	11	16	18	11	37	13	11.9	5.0	6.4
Ni	103	58	20	10	12	9	15	12	21	21	72	35	38	43	16	3	
Cr	157	81	41	26	34	22	21	19	50	111	128	85	50	58			12
V	184	50	95	31	39	24	43	26	52	32	95	19	129	44	25	6	47
La	41.1	15	19.2	8	35.3	19	31.4	25	30.8	24	59.9	28	90.9	46	28.65	10.80	8.70
Ce	89.8	30	37.7	16	61.7	33	55.1	35	58.5	400	126	47	188	80	53.56	16.26	16.20
Nd	47.1	16	18.2	7	25.8	14	19.6	14	23.2	19	54.8	16	84.9	34	25.05	4.04	11.40
Sm	7.8	2.5	3.4	1.3	4.2	2	3.3	3	3.5	2	9.8	3	14.5	6			3.40
Eu	2.0	0.6	0.9	0.3	1.0	0.39	0.8	0.36	0.9	0.45	2.3	0.62	3.2	1.09	1.23	0.21	
Gd	4.8	1.3	2.8	0.8	3.2	2.2	2.4	1.3	2.3	1.4	6.0	1.4	9.2	2.1			
Dy	2.8	0.7	1.9	0.5	1.8	1.1	1.9	1.0	1.6	0.9	3.2	0.8	5.6	1.1	2.35	0.93	2.60
Er	1.21	0.3	0.96	0.3	0.77	0.7	0.77	0.4	0.75	0.5	1.41	0.5	2.68	0.7	1.21	0.61	1.30
Yb	0.93	0.2	0.88	0.2	0.78	0.4	0.63	0.4	0.63	0.4	1.32	0.7	2.05	0.8	0.94	0.59	1.10
Lu	0.08	0.03	0.17	0.04	0.20	0.12	0.13	0.1	0.12	0.1	0.26	0.1	0.34	0.1			
K_2O/Na_2O	0.58		0.47		0.44		0.38		0.43		0.63		0.80		0.51		
Mg#	0.61		0.48		0.38		0.41		0.45		0.57		0.48		0.40		
Sr/Y	162.21		55.65		30.45		31.44		51.10		63.98		26.58		28.04		
(La/Yb)N	29.32		14.44		29.85		32.86		32.52		29.92		29.32		20.18		

Average experimental melt composition is from Zamora (2000) and pristine melt from Rapp and Watson (1995).

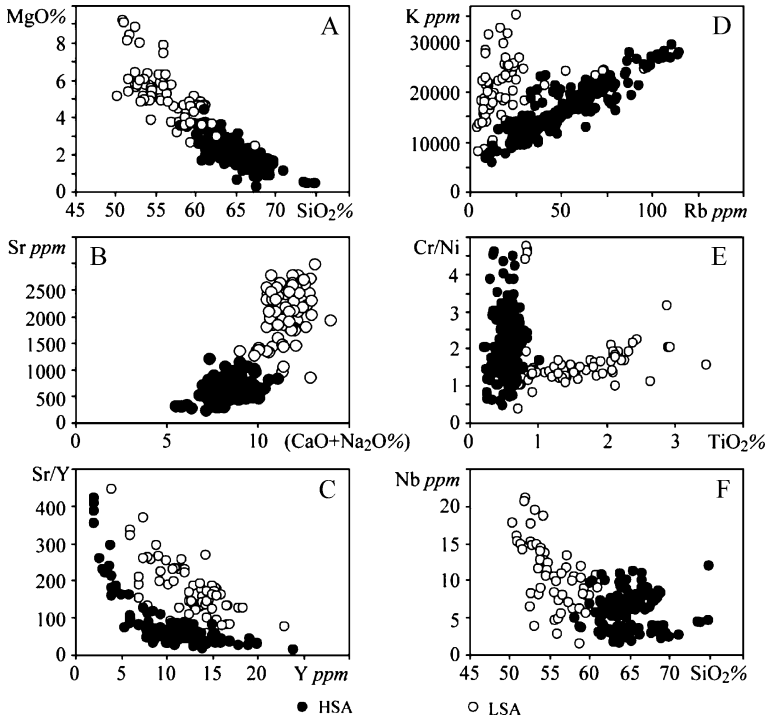

Fig. 1. MgO vs. SiO_2 (A); Sr vs. ($CaO+Na_2O$) (B); (Sr/Y) vs. Y (C); K vs. Rb (D); (Cr/Ni) vs. TiO_2 (E); and Nb vs. SiO_2 (F) diagrams comparing high-SiO_2 adakites (HSA; ●) and low-SiO_2 adakites (LSA; ○).

between slab-melts and mantle peridotite. Mantle xenoliths in volcanic rocks from Kamchatka (Kepezhinskas et al., 1995, 1996) are crosscut by MgO and Cr-enriched adakitic veins. At the contact with the adakite veins, the mantle consists of a metasomatised peridotite made up of garnet, Al-pyroxene, pargasitic amphibole, and Na-rich plagioclase. These relationships not only show the effect that mantle interaction has on adakite but also the important corresponding metasomatic effects that the slab-melt has on mantle peridotite.

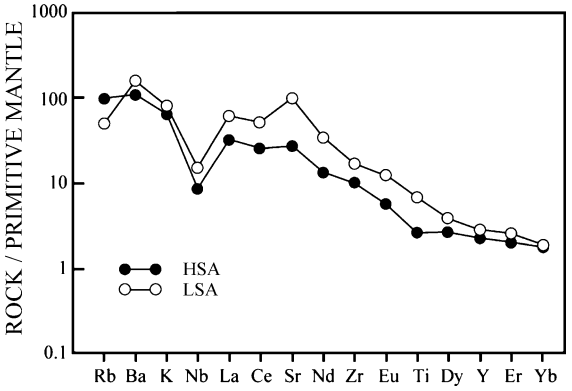

Fig. 2. Primitive mantle (McDonough et al., 1992) normalized multielement diagram for average compositions of LSA (○) and HSA (●). LSA differs from HSA by its positive Sr anomaly, its relative Rb depletion, as well as by its higher Nb and REE contents. HSA has lower Ti content than LSA and shows a slight negative anomaly.

Recently, the interaction of felsic magma with mantle peridotite has been experimentally investigated (Kelemen et al., 1990; Rapp et al., 1999; Prouteau et al., 2001). Based on these experiments, Rapp et al. (1999) established the concept of "effective melt/rock ratio". As is shown by the natural examples from Kamchatka, slab-melt not only assimilates mantle peridotite but also metasomatises peridotite, and in so doing, it is progressively consumed. When the melt/rock (i.e., slab-melt/peridotite) ratio is high, not all slab-melt is consumed during peridotite metasomatism and so contaminated melt (adakite) may reach the surface. When the melt/rock ratio is low, all the slab-melt is consumed in metasomatic reaction with the

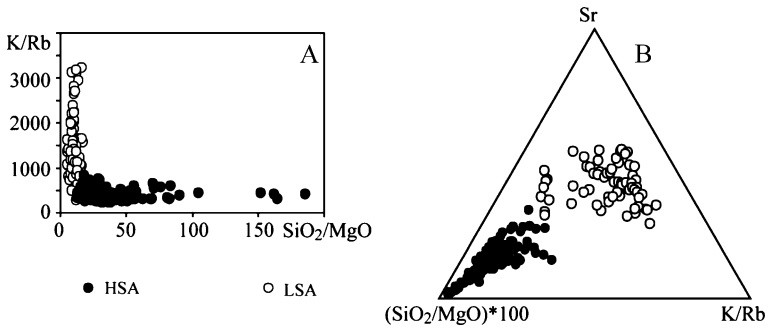

Fig. 3. (K/Rb) vs. (SiO_2/MgO) plot and Sr–(K/Rb)-(SiO_2/MgO)×100 triangular diagrams. These diagrams best discriminate between HSA (●) and LSA (○). Average compositions are from Table 1.

peridotite. This is probably the situation for the Batan Islands where adakite forms inclusions in peridotite nodules but where no adakite is erupted at the surface (Schiano et al., 1995). Subsequent melting of this metasomatised peridotite, however, produces magmas that retain a strong slab-melt signature. Thus, depending on the effective melt/rock ratio, there are at least two petrogenetic scenarios whereby magmas with a strong slab-melt influence can form. These two scenarios represent the differences between slab-melt contaminated by peridotite and magma derived from peridotite contaminated by slab-melt. Whether or not both petrogenetic scenarios should be encompassed within a strict definition of adakite, we suggest they reflect the difference respectively between HSA and LSA. We illustrate our point below using a range of key trace elements.

2.2.2. Sr concentrations

High Sr and low Y concentrations, and correspondingly high Sr/Y ratios are generally considered as defining characteristics of adakite that reflect their high-pressure, slab-melt origins (Defant and Drummond, 1990; Drummond and Defant, 1990). Fig. 1B shows that Sr concentrations vary in a wide range up to 1100 ppm in HSA and from 1000 to 3000 in LSA. Sr concentration in melts is mainly dependent on Sr content in the basaltic source. However, during melting of the same basalt source, the degree of Sr enrichment in melt will be mostly controlled by residual plagioclase (Kd_{Sr}=0.35 to 1.5; Rollinson, 1993). Since the stability of plagioclase is strongly pressure-dependent, so too is the concentration of Sr in melts derived from basalt. This was demonstrated by Zamora (2000) who performed extensive experiments on a single oceanic basalt containing 88 ppm Sr. He determined 53 glass compositions for a wide range in both temperature (850–1150 °C) and pressure (7–35 kbar). Fig. 5 is a Sr_{Melt}/Sr_{Source} vs. Na_2O+CaO diagram where the degree of Sr-enrichment in the melt

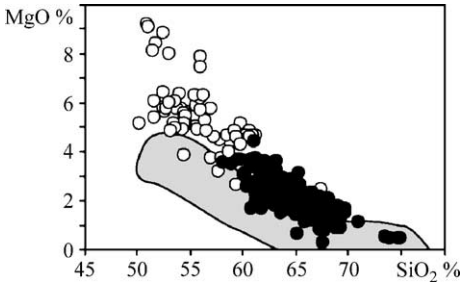

Fig. 4. MgO vs. SiO_2 plot comparing experimental melts composition (grey field) with both HSA (●) and LSA (○). For the same SiO_2 content HSA and to a greater extent, LSA are richer in MgO than experimental melts.

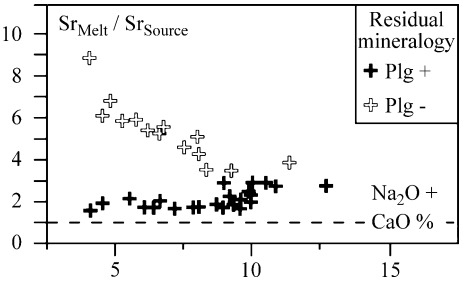

Fig. 5. Diagram showing the degree of enrichment of Sr (Sr_{melt}/Sr_{source}) in experimental melts as a function of (Na_2O+CaO). When plagioclase is a residual phase (black crosses) the degree of enrichment remains low, whereas when plagioclase is not stable during fusion (white crosses), the degree of enrichment can reach 9 times the source content. Data are from Zamora (2000).

is quantified by the Sr_{Melt}/Sr_{Source} ratio. Here, the composition of experimental glasses in equilibrium with a plagioclase-bearing residue (black crosses) is compared with those in equilibrium with a plagioclase-free residue (white crosses). Residual plagioclase buffers the Sr concentration in the liquid at about 1.5 to 2 times the concentration in the basaltic parent, significantly lower than concentrations in either HSA or LSA. However, when plagioclase is absent, the degree of enrichment can reach 9 times. Na_2O+CaO do not show exactly the same behaviour as Sr because of the additional control that amphibole, clinopyroxene, and garnet can exert over these elements.

Nevertheless, using the partition coefficients given by Rollinson (1993), simple calculations show that 15% to 25% partial melting of a typical basaltic composition containing 100 to 200 ppm Sr (i.e., N-MORB to E-MORB concentrations), leaving a plagioclase-free residue, cannot generate magmas with more than 1000 ppm Sr. This may account for concentrations in HSA but not in LSA. However, the same calculation, assuming 5% to 10% melting of a peridotite with 25 ppm Sr, and contamination by addition of 20% slab-melt with 700 ppm Sr, can generate magmas containing 1500 to 2500 ppm Sr. Consequently, the very high Sr content considered as typical of adakites is probably only characteristic of LSA and, as already proposed for orogenic granites (Tarney and Jones, 1994), is more consistent with a metasomatised mantle origin rather than with a pure slab-melt.

2.2.3. Nb concentrations

Fig. 1F shows that, while HSA and LSA have similarly low Nb concentrations, LSA concentrations extended to greater than 10 ppm. For both adakite groups, mantle normalized multi-element diagrams show negative Nb (Fig. 2) and Ta anomalies when compared to K and La (Fig. 2; Maury et al., 1996; Martin, 1999). This behaviour is classically interpreted as reflecting the residual behaviour of minerals like rutile during basalt melting ($Kd^{rut/liq}$ for Nb and Ta are >20; Green and Pearson, 1987; Foley et al., 2000). However, rutile fractionation should also cause a strong negative Ti anomaly, and this is not always the case in adakite. Rather, Drummond and Defant (1990) proposed that amphibole, whose $Kd^{amp/liq}$ for Nb–Ta in intermediate to felsic liquids is ~4 (Pearce and Norry, 1979; Lemarchand et al., 1987), could be the cause of negative Nb-Ta anomalies in adakite. It must be noted that more recently, Kd<1 were reported for Nb–Ta between amphibole and liquid (Adam et al., 1993; Klein et al., 1997). This hypothesis is very attractive, as amphibole is likely to play a role during basalt melting as well as during subsequent fractional crystallization. On the other hand Rapp and Watson (1995) and Rapp et al. (2003) show that amphibole does not necessarily play a prominent role, as basalt melting experiments leaving a rutile-bearing eclogite residue do not always produce a negative Ti anomaly, whereas strong Nb and Ta negative anomalies are always observed.

The typically higher Nb contents of LSA liken these rocks, in some respects, to high-Nb basalts (HNB; Nb≥20 ppm; Regan and Gill, 1989; Defant et al., 1992) or more precisely with niobium-enriched basalts (NEB; 7 ppm<Nb<<20 ppm; Defant et al., 1992; Maury et al., 1996; Sajona et al., 1996). These latter authors propose that NEB result from melting of a mantle peridotite previously metasomatised and enriched in Nb by slab-melts. In a typical subduction zone, the mantle wedge is metasomatised by fluids derived from the dehydration of the subducted slab. These fluids cannot concentrate Nb or Ta (Tatsumi et al., 1986; Tatsumi and Nakamura, 1986), which remain in the subducted slab, accounting for the Nb–Ta depletion (with respect to La) typical of classic arc magmas. Slab-melt, in contrast, is able to transfer Nb and Ta into the wedge. Indeed, the average Nb content in adakites is ~6 ppm whereas mantle values are typically <1 (Taylor and McLennan, 1985). Consequently, while the Nb content in HSA is consistent with slab-melting, higher Nb content in LSA better fits with melting of peridotite previously metasomatised by slab-melt.

2.2.4. Ti concentrations

TiO_2 content in HSA is always lower than 0.9% whereas it can be greater than 3% in LSA (Fig. 1E). All experiments performed on basalt melting showed that ilmenite or rutile are always residual phases (Rapp et al., 1991; Rapp and Watson, 1995; Zamora, 2000, among others). Such residual assemblages should buffer melt Ti concentrations at low values. If this is the case, the high-Ti concentrations of LSA precludes the presence of Ti-rich phase in melting residues, in contrast with experimental slab-melts. However, high-Ti concentrations are common in the

products of mantle peridotite melting, as shown (for example) in oceanic islands magmas and also in arc magmas such as those from the Central Volcanic zone of the Andes (Thorpe et al., 1984; Wilson, 1991).

2.2.5. Cr/Ni ratio

Fig. 1E shows that the Cr/Ni ratio can also efficiently discriminate some HSA (Cr/Ni 0.5 to 4.5) from LSA (Cr/Ni 1 to 2.5). The Cr/Ni ratio of MORB ranges between 2.4 and 4.5. All residual phases during basalt melting have $Kd_{(Cr/Ni)}^{min/liq}>2$ (Rollinson, 1993), thus resulting in a decrease of Cr/Ni in magmas during partial melting. Moreover, the Cr/Ni ratio in HSA is positively correlated with Mg#, which indicates that the Cr/Ni ratio is a parameter dependent on fractionation.

The low Cr/Ni ratios and narrow range shown by the LSA indicates a source that is not basaltic. Mantle peridotites have Cr/Ni around 1.5 (Taylor and McLennan, 1985; McDonough and Sun, 1995), which is the average value in LSA. During melting, several residual phases have $Kd_{(Cr/Ni)}^{min/liq}$ greater than one (orthopyroxene=2; clinopyroxene=3, garnet=3.6) but their effect is buffered by olivine ($Kd_{(Cr/Ni)}^{min/liq}$~0.1; Rollinson, 1993), which is the main residual phase during mantle melting, resulting in a D equal or slightly greater than 1. Thus, the range of Cr/Ni ratios in LSA is also consistent with mantle peridotite melting. Possible metasomatism of mantle peridotite by adakitic melts should not significantly modify this ratio as the $Cr_{peridotite}/Cr_{adakite}$ and $Ni_{peridotite}/Ni_{adakite}$ are very high (10 and 20, respectively).

2.2.6. K and Rb concentrations

The K/Rb ratio can be up to four times greater in most LSA than in HSA. It appears that this is mainly due to low Rb concentrations in LSA because K concentrations are roughly similar in both groups. In oceanic basalts, the K/Rb ratio is typically around 1000. Residual minerals during melting of basaltic material have $Kd_{(K/Rb)}^{min/liq}>1$ (amphibole=6, clinopyroxene=1, garnet=20; Rollinson, 1993) and so the melts should have K/Rb<1000. This is clearly the case for HSA (K/Rb=250). Both K and Rb, however, are strongly incompatible in minerals residual from peridotite melting (olivine, orthopyroxene, clinopyroxene, and garnet), and so mantle values (~350) should not be strongly fractionated during melting. The extreme Rb depletion observed in adakites from Mexico has been attributed to the presence of metasomatic amphibole in a peridotitic source (Rogers et al., 1985; Calmus et al., 2003). Metasomatism of mantle peridotite by slab-melts produces orthopyroxene, clinopyroxene, garnet, phlogopite, and richterite or pargasite (Sen and Dunn, 1994a; Rapp et al., 1999; Prouteau et al., 2001). Schmidt and Poli (1998) showed that during melting of such an assemblage, amphibole melts first at 980–1000 °C whereas phlogopite melts at greater temperature (1150 °C). The amphibole melting reaction produces clinopyroxene (10%), garnet (30%), and melt (60%) (Francis and Ludden, 1995; Dalpé and Baker, 2000). Ionov and Hofmann (1995) have shown from mantle xenoliths that amphiboles can have high K and very low Rb concentration while coexisting phlogopite is rich in both K and Rb. Thus, selective melting of amphibole would account for low Rb content and correlated high K/Rb in LSA. Here, too, it is suggested that the pargasite-bearing mantle source has been metasomatised by slab-melt (Calmus et al., 2003).

2.3. Petrogenesis

2.3.1. HSA

When plotted together with adakites, experimental liquids obtained by basalt or amphibolite melting systematically plot together with HSA (Fig. 6). The trace element data from Zamora (2000) correspond to melts in equilibrium with a garnet-bearing residue. No Cr measurements are available on experiments, and so the Cr/Ni vs. TiO_2 plot cannot be presented. However, the average TiO_2 content of experimental melts is 0.7 wt.% (σ=0.5), which is consistent with the range of HSA. Only small differences are observed when MgO, Cr, and Ni are taken into consideration. We consider that the geochemical relationships outlined in the previous section, and the close compositional similarities between analytical data, geochemical modelling, and experimental data provide a compelling case that HSA have formed by melting of a basaltic material, and at a pressure high enough to stabilize garnet (i.e., eclogite or garnet amphibolite). The HSA series evolve from hornblende bearing andesite to dacite or rhyolite; it is not known to include basaltic members. Pyroxene phenocrysts are never found. Partial melting of a

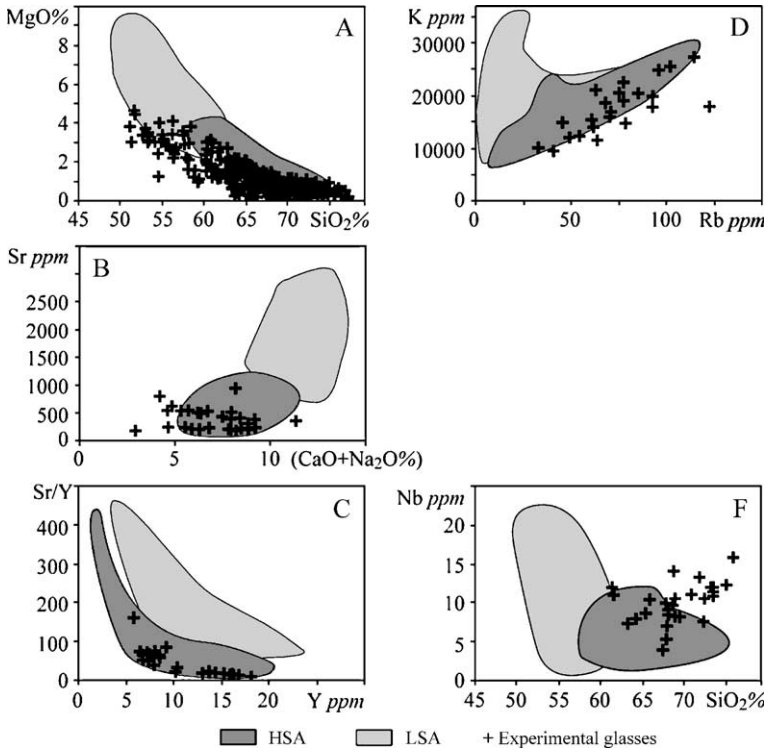

Fig. 6. MgO vs. SiO_2 (A); Sr vs. ($CaO+Na_2O$) (B); (Sr/Y) vs. Y (C); K vs. Rb (D); and Nb vs. SiO_2 (F) diagrams comparing high-SiO_2 adakites (HSA; dark grey field) and low-SiO_2 adakites (LSA; light grey field) with liquids obtained by experimental melting of basalts (crosses). As no Cr measurement is available from the experiments, the Cr/Ni vs. TiO_2 plot cannot be presented. Only HSA have compositions consistent with experimental liquids.

basalt will necessarily produce intermediate to felsic magmas and so these observed petrological and mineralogical characteristics of the HSA suites are also consistent with an origin through basalt melting.

However, MgO, Cr, and Ni concentrations in HSA are clearly higher than in experimental melts. As already discussed, several authors (Maury et al., 1996; Stern and Kilian, 1996; Rapp et al., 1999; Smithies, 2000; Prouteau et al., 2001) interpret these differences as reflecting interactions between basalt melt and peridotite. In other words, their genesis occurred by basalt melting at great depth and under a significant mantle thickness that allowed substantial interaction. These conclusions are reinforced by the discovery of glass inclusion in olivine crystals from mantle peridotite xenolith from the Batan subduction zone (Schiano et al., 1995).

As HSA have all come from active subduction zones, basalt melting must have also occurred in this kind of environment. Although widely believed to result, in this environment, from slab-melting (Stern and Futa, 1982; Defant and Drummond, 1990; Drummond and Defant, 1990; Rapp et al., 1991; Peacock et al., 1994; Morris, 1995; Maury et al., 1996; Prouteau et al., 1996; Stern and Kilian, 1996; Sigmarsson et al., 1998; Martin, 1999; Rapp et al., 1999; Bourdon et al., 2002; Samaniego et al., 2002), it has also been suggested that some adakites may result through melting of basalts underplated beneath continental crust (Atherton and Petford, 1993; Mahlburg Kay et al., 1993; Petford and Gallagher, 2001; Garrison and Davidson, 2003). Melting of underplated basalt should not normally allow interaction between the felsic melts and mantle peridotite, and so this cannot be a general model for adakite (HSA) petrogenesis. Basalt melting experiments performed by Prouteau et al. (2001) indicated that trondhjemitic melts are only generated when free water is available,

whereas dehydration melting gives rise to less-sodic compositions. Dehydration melting, rather than hydrous melting, is more likely the case for underplated basalt and so suites generated in this way should lack trondhjemitic compositions. Trondhjemite, by contrast, is an important component of HSA suites.

2.3.2. LSA

LSA lavas sometimes contain pyroxene, as phenocrysts; they are basaltic to andesitic in composition, and consequently possess compositions incompatible with basalt melting. Both major and trace element compositions are consistent with an origin by partial melting of a mantle peridotite. As LSA are all generated in active subduction zones, the problem of their genesis could appear as quite trivial because most calc–alkaline magmas are generated in subduction environments by melting of a metasomatised mantle. However, in classical calc–alkaline magmatism, fluids derived from slab dehydration are the metasomatic agents. The resulting magmas are LILE (K)-rich, Nb–Ta-depleted, and have high HREE contents. In the case of LSA, the K_2O/Na_2O ratio remains low, Nb and Ta are not systematically depleted and may even be enriched, Sr contents are very high, and HREE content are very low. As discussed earlier, these characteristics more reasonably fit with a mantle peridotitic source metasomatised by slab-melts.

The average Yb content in LSA is 0.93 ppm whereas it is 4.4 ppm in typical arc dacite. In a mantle peridotite, all potential residual minerals have $Kd_{Yb}^{min/liq} \ll 1$ such that Yb behaves as a very incompatible element. This is obviously true for classic arc dacites which are Yb-enriched when compared to their peridotite source that typically has about 0.37 ppm Yb (Taylor and McLennan, 1985). Slab-melts are characterized by low Yb-contents and so metasomatism will not significantly modify mantle peridotite composition. Consequently the low HREE content of LSA reflects the role played by minerals with $Kd_{(HREE)}^{min/liq} > 1$. One of these minerals is garnet which is stable in peridotite at high pressure. Garnet is the only commonly available mantle phase that can enrich magma in LREE and deplete it in HREE (i.e., strongly fractionated REE patterns). However, garnet is consumed (i.e., is not a residual phase) after only small degrees of melting-this is probably the case in classic arc magmas. In the case of peridotite that has been metasomatised by slab-melt, the situation can be quite different. Firstly, Prouteau et al. (2001) has shown that metasomatism via a slab-melt is more than 15 times more efficient than fluid mediated metasomatism and is thus more likely to result in extensive conversion of peridotite to the metasomatic assemblage pyroxene+garnet+amphibole+phlogopite. During subsequent melting of this assemblage, amphibole melts first, producing garnet and clinopyroxene in a ratio of 3:1 (Francis and Ludden, 1995; Dalpé and Baker, 2000). In such a case, garnet can remain stable over degrees of melting sufficiently wide to generate HREE depleted magmas like LSA. It must be noted that in this situation, the adakitic signature of LSA is indirectly related to slab-melts (whose mixing with, or interaction or assimilation by, mantle would not modify the HREE budget) through metasomatic reactions that allow garnet to remain stable during a wider range of melting.

2.3.3. Summary

The difference pointed out between HSA and LSA is not simply a subtle difference in mineralogy or in chemistry or an artefact of classification. Rather, it reflects a fundamental difference in petrogenesis, and specifically in different sources. HSA are the direct result of melting subducted hydrated basalt and variably contaminating those slab-melts by peridotite assimilation as they ascend through the mantle wedge. LSA are generated in two distinct episodes; complete consumption of slab-melt during melt–peridotite interaction, followed by melting of this metasomatised peridotite source. The unifying petrogenetic feature of these magmas is that both are directly or are indirectly linked to slab-melts. The same petrogenetic feature may link them to Archaean TTG and sanukitoids.

3. Archaean TTG

3.1. Definition

About 90% of the juvenile continental crust generated between 4.0 and 2.5 Ga belongs to ‘TTG suites’ (tonalites, trondhjemites, and granodiorites; Jahn et al., 1981; Martin et al., 1983), although in

some cratons (e.g., Yilgarn; Sylvester, 1994; Champion and Sheraton, 1997), high-K monzodioritic and syenogranitic rocks can be abundant. Typical TTG are equigranular quartz+plagioclase+biotite-bearing plutonic rocks: K-feldspar, where present, forms only a minor component whereas the more primitive members of the suites can be hornblende-rich. Accessory phases are allanite, pistacite, apatite, zircon, sphene, and titanomagnetite.

TTGs are silica-rich (SiO_2>64 wt.%, but, commonly, ~70 wt.% or greater) with high Na_2O contents (3.0 wt.%≤Na_2O≤7.0 wt.%) and correlated low K_2O / Na_2O (<0.5), with no K-enrichment during magmatic differentiation (Table 1 and Fig. 7). They are poor in ferromagnesian ($Fe_2O_3^*$+MgO+MnO+TiO_2<5 wt.%), with an average Mg# of 0.43 and average Ni and Cr contents of 14 and 29 ppm, respectively (Martin, 1994). Barker and Arth (1976) subdivided Archaean sodic (trondhjemitic) granites into two groups—high-Al and low-Al groups. The high-Al group is characterised by elevated Sr and Eu and low Yb and Y contents, strongly fractionated REE patterns ($(La/Yb)_N$ up to 150) and high Sr/Y ratios. These features are interpreted as reflecting the presence of garnet and amphibole as well as the lack of plagioclase, either as residual or fractionating phases. The low-Al group, with lower Sr and Eu contents, less fractionated REE and lower Sr/Y ratios, reflects a petrogenesis that did not involve garnet, but was controlled by plagioclase, either as a residual or fractionating phase. Most TTGs belong to the high-Al group (Martin, 1994) and, as pointed out by Champion and Smithies (2003a), a high-pressure origin has become implicit in the term 'Archaean TTG'. Unless otherwise stated, our reference to TTG here applies only to high-Al TTG. Importantly, Figs. 8 and 9 show that there is an extremely high degree of compositional overlap between TTG and HSA in terms of nearly all major and trace elements, supporting the widely held view that these rocks share many petrogenetic similarities.

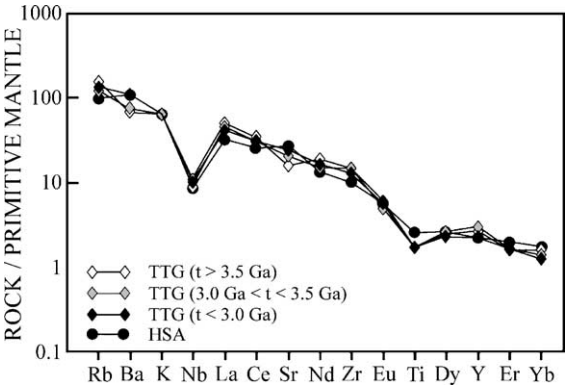

Fig. 8. Primitive mantle (McDonough et al., 1992) normalized multi-element diagram for average HSA (●) compared with TTG of different ages (black diamond=average TTG<3.0 Ga; grey diamond=3.0 Ga<average TTG<3.5 Ga; white diamond=average TTG>3.5 Ga). Patterns for HSA are very similar to those for TTG irrespective of age. Average compositions are from Table 1.

3.2. Petrogenetic models

As is the case for HSA, comparisons of Archaean TTG to geochemical models and to the results of experimental high-pressure melts of hydrous basalt, have led to the conclusion that TTG formed via low to moderate degree partial melting of hydrated basaltic (low-K) crust at pressures high enough to stabilize garnet±amphibole (i.e., eclogite or garnet amphibolite; Arth and Hanson, 1975; Barker and Arth, 1976; Tarney et al., 1979; Condie, 1981;

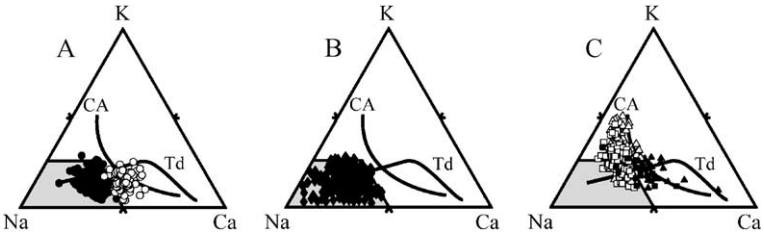

Fig. 7. K–Na–Ca triangles: (A) adakites (LSA (○); HAS (●)); (B) TTG (♦); and (C) sanukitoids (SiO_2>62% (□); SiO_2<62% (■)), Closepet-type granites (SiO_2>62% (△); SiO_2<62% (▲)), and Trends are from Barker and Arth (1976). Td=trondhjemitic differentiation trend; CA=classical calc–alkaline trend. In grey: field of Archaean TTG (Martin, 1994).

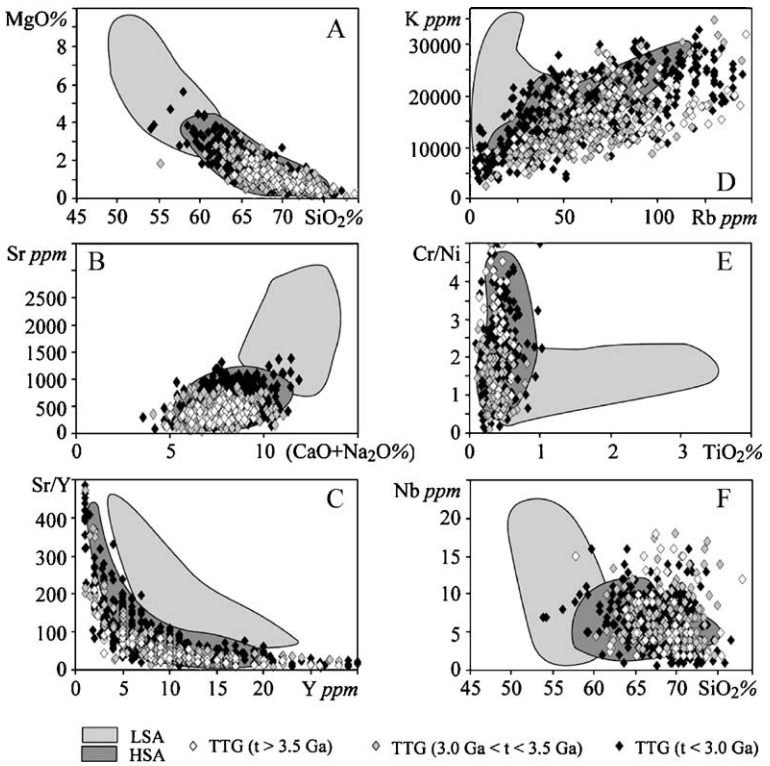

Fig. 9. MgO vs. SiO_2 (A); Sr vs. (CaO+Na_2O) (B); (Sr/Y) vs. Y (C); K vs. Rb (D) ; (Cr/Ni) vs. TiO_2 (E); and Nb vs. SiO_2 (F) diagrams comparing high-SiO_2 adakites (HSA; dark grey field) and low-SiO_2 adakites (LSA; light grey field) with TTG of different ages (black diamond=TTG<3.0 Ga; grey diamond=3.0 Ga<TTG<3.5 Ga; white diamond=TTG>3.5 Ga). Only HSA have compositions very similar to TTG younger than 3.0 Ga.

Tarney et al., 1982; Martin, 1986, 1987; Rapp et al., 1991; Rapp and Watson, 1995). The lack of mafic end-members to the TTG suites indicates that partial melting, rather than fractional crystallization, was the dominant process. More recently, Foley et al. (2002) have argued that only an amphibolitic source is able to account for the typically low Nb/Ta and high Zr/Sm ratios of TTG. Nevertheless, their systematically low HREE concentrations and normalised Gd/Yb>1 still point to a garnet-bearing source (garnet-bearing amphibolite). In addition, Rapp et al. (2003) show that similar ratios can also result through partial melting of hydrous arc-related mafic crust leaving an eclogitic residue.

The apparent high pressures required for TTG genesis and the compositional similarities with adakites (Fig. 8) known to have formed in subduction environments have led to the conclusion that TTG also formed via melting of subducted oceanic crust (Martin, 1986, 1999). Archaean heat production was 2–4 times greater than today (Brown, 1985) and, consequently, Archaean geotherms were significantly greater than typical modern geotherms (e.g., Bickle, 1986). During the Archaean, the 'normal' thermal regime was probably quite similar to that observed at today's zones of 'hotter' subduction, where adakite has typically been produced. Such comparisons clearly invite a subducted-slab-melt model for TTG. However, the idea that adakite is invariably a petrogenetic analogue for all TTG has recently been challenged. Based on secular changes in TTG compositions, Smithies (2000) and Smithies and Champion (2000) proposed that alternative processes such as melting of tectonically or magmatically thickened hydrous mafic crust (e.g., Davies, 1992; Atherton and Petford, 1993; De Wit, 1998) might be more appropriate for Early Archaean TTG.

3.3. Change in TTG composition through time

Recently, Smithies (2000), Smithies and Champion (2000), and Martin and Moyen (2002) showed that the chemical composition of TTG has changed through Archaean times. Throughout that time, the most remarkable change was a decrease in average SiO_2 and an increase in average MgO content (Figs. 9 and 10). According to Martin and Moyen (2002), the Mg# of the more primitive TTG magmas increased from maximum values of 0.45 at 4.0 Ga to 0.65 at 2.5 Ga (Fig. 11). These authors also pointed out that over the same time interval the maximum concentrations of Ni increased from ~30 to ~70 ppm, Cr from ~50 to ~200 ppm, Sr from ~550 ppm to ~1200 ppm, and (Na_2O+CaO) increased from 9 to 11 wt.%. Fig. 8 also shows that TTG older than 3.5 Ga have a negative Sr anomaly, whereas the anomaly is slightly positive in TTG younger than 3.0 Ga (Fig. 8). Considering elements other than Sr, Ba, Ni, Cr, and Mg, the close similarities in the compositional range for TTG is independent of age, and suggests a common petrogenetic relationship that is also age independent. We propose that only the details of this mechanism, and/or the behaviour of magma after its genesis, changed.

The Mg# of some TTGs, especially the younger (ca <3.0 Ga), is higher than values determined by experimental high-pressure melting of basaltic material. As for adakites, these higher Mg# are interpreted in terms of interaction of TTG parental magma with mantle wedge peridotite (e.g., Maury et al., 1996; Rapp et al., 1999; Smithies, 2000; Martin and Moyen, 2002). As shown by Figs. 8 and 9, the compositions of these younger TTGs and of modern HSA are very similar, and so their petrogenesis is also likely to be similar. The significantly lower mean Mg#, Cr, and Ni in Early Archaean (>3.3 Ga) TTG, however, is interpreted to reflect less-efficient interactions between TTG parental magma and peridotite (Smithies, 2000; Martin and Moyen, 2002). Although Martin and Moyen (2002) and Smithies et al. (2003) disagree in detail about the nature of these changes (i.e., progressive vs. more punctuated), a consensus is that, before ~3.3 Ga, the efficiency of interactions, if any, between TTG parental magma and mantle peridotite was very low and certainly significantly less than it was during the Late Archaean. For this reason, Smithies (2000) proposed that the petrogenesis of Early Archaean TTGs was not analogous to that of modern adakite.

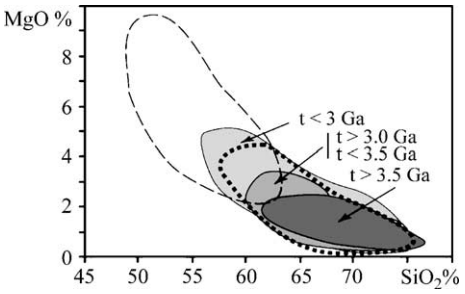

Fig. 10. MgO vs. SiO_2 diagram comparing composition of TTGs at different times (grey fields) with modern HSA (heavy dotted lined field) and LSA (light dotted lined field). A close analogy exists only between TTG younger than 3.0 Ga and HSA.

The fact that Early Archaean TTG did not significantly interact with mantle peridotite has important implications in terms of Archaean crustal evolution and dynamics. Two mechanisms, directly

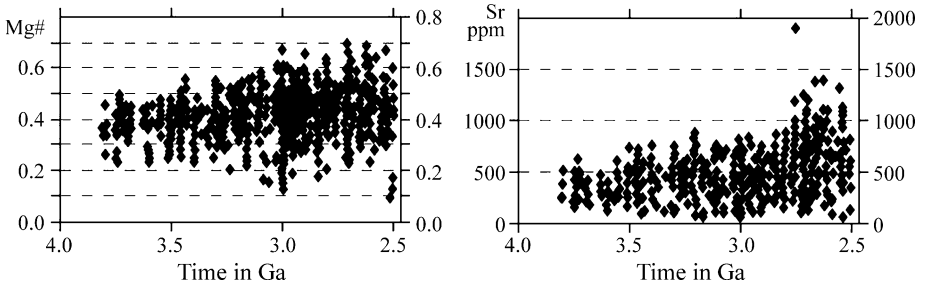

Fig. 11. Diagrams showing time-evolution of Mg# and Sr in TTG magmas during the Archaean (Martin and Moyen, 2002). The upper envelope of the group of points represents the composition of the more primitive TTG magmas.

related to the higher inferred Archaean heat flow may be proposed:

(1) Based on Sr and (Na_2O+CaO) variations in TTG parental magmas (Fig. 11), Martin and Moyen (2002) proposed that the depth of slab-melting progressively increased from Early to Late Archaean. The concentrations of Sr and (Na_2O+-CaO) in TTG magmas strongly depends on presence or absence of residual plagioclase during hydrous basalt melting (Fig. 4), and hence, on pressure. At >3.5 Ga heat flow was high, such that slab-melting occurred at shallow depth (plagioclase was stable, TTG are Sr-poor). As a result, the column of mantle wedge through which the slab-melt had to ascend was very short and so interaction between the slab-melt and peridotite was limited. However, by 2.5 Ga, when the heat flow was lower, slab-melting occurred at a greater depth (plagioclase not more stable, TTG magmas are Sr-rich) and felsic magmas strongly reacted with the thicker mantle wedge peridotite.
(2) Alternatively, Smithies et al. (2003) propose that, before ~3.3 Ga, the relationship between heat flow and oceanic crust thickness (e.g., Bickle, 1986; Davies, 1992; Abbott et al., 1994) was such that where oceanic crust could be subducted, its greater thickness and buoyancy resulted in a very low angle of subduction (flat subduction) that prevented any effective mantle wedge forming. Melting of the subducted slab would have resulted in TTG magmas that never interacted with mantle material. As shown by Gutscher et al. (2000a,b), modern flat subduction also favors adakite genesis.

These two models are not mutually exclusive—it seems likely that the warmer Early Archaean Earth worked in at least two complementary ways to ensure that interaction between slab-melts and mantle peridotite was not a dominant process before ca. 3.3 Ga.

3.4. TTG vs. HSA and LSA

Figs. 7 and 9 show that LSA are essentially without any compositional analogue in the TTG suite. By contrast, HSA show an extensive compositional overlap with TTGs (Fig. 9B). Importantly, these comparisons strongly suggest that the petrogenesis of TTG is unlikely to involve significant primary melting of metasomatised mantle peridotite (like HSA) they are melts of hydrated basalt.

Consequently, we consider that HSA is a reasonable petrogenetic analogue for Middle to Late Archaean TTG. By contrast, most Early Archaean TTGs differ from these two groups of rocks in that they have systematically lower Mg#, Cr, and Ni and higher SiO_2. While the primary basaltic source for all these rocks may not differ, these seemingly small compositional differences have significant implications both in terms of petrogenesis (i.e., no effective mantle wedge) and of crustal geodynamic evolution models. There appear to be no suites of modern adakites that are direct compositional or petrogenetic analogues of >3.5 Ga TTG.

4. Sanukitoids and Closepet-type granites

4.1. Definition

Shirey and Hanson (1984) first recognized a suite of Late Archaean felsic intrusive and volcanic rocks from the Superior Province that contrasted in composition from the TTG suite. Because the major element geochemistry of these rocks resembles that of Miocene high-Mg andesite (sanukite) from the Setouchi volcanic belt of Japan (e.g., Tatsumi and Ishizaka, 1982), Shirey and Hanson (1984) referred to them as 'Archaean sanukitoids'. Sanukitoids are now generally regarded as a minor, although widespread, component of most Late Archaean terranes, having been documented from the Superior Province (Shirey and Hanson, 1984, 1986; Stern and Hanson, 1991; Stevenson et al., 1999), Baltic shield (Querré, 1985; Lobach-Zhuchenko et al., 2000a,b, 2005; Samsonov et al., 2005), South India (Balakrishnan and Rajamani, 1987; Krogstad et al., 1995; Sarvothaman, 2001; Moyen et al., 2003a), and the central Pilbara Craton (Smithies and Champion, 1999a).

A more recently identified rock suite that shares several characteristics of sanukitoids is the Late Archaean Closepet-type Granite, so far reported only from South India (Jayananda et al., 1995; Moyen et

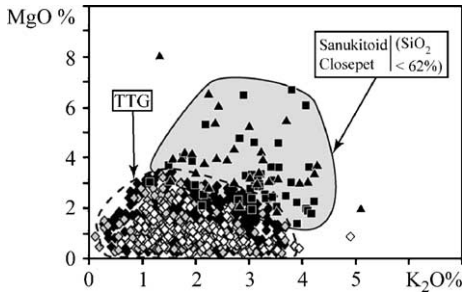

Fig. 12. MgO vs. K_2O plot comparing TTG (black diamond= TTG<3.0 Ga; grey diamond=3.0 Ga<TTG<3.5 Ga; white diamond= TTG>3.5 Ga) with Archaean sanukitoids (■) and Closepet-type granites (▲) whose SiO_2 content is lower than 62%. Sanukitoids and Closepet type granites differ from TTG in having higher MgO and K_2O contents.

al., 2001, 2003b). However, some plutons from Wyoming (Frost et al., 1998), Shandong, China (Jahn et al., 1988), and Limpopo (Barton et al., 1992) also show Closepet-type compositions. The petrogenesis of sanukitoids and of Closepet-type granites is generally interpreted to be very similar, and accordingly, these suites are considered together here. Intrusion of sanukitoid and Closepet-type granite is commonly late- to post-kinematic (e.g., Shirey and Hanson, 1984; Stern, 1989; Evans and Hanson, 1997; Beakhouse et al., 1999; Smithies and Champion, 1999b) and is generally not temporally associated with TTG magmatism. Very often they constitute one of the last magmatic events in an already cratonized continental crust. All are plutonic and locally feldspar porphyritic rocks. Sanukitoid suite composition ranges from dioritic to granodioritic (tonalite being subordinate), whereas Closepet-type can evolve to monzogranitic compositions. In contrast to the TTG series, sanukitoid and Closepet-type granite can be rich in mafic minerals, commonly including biotite+-hornblende±clinopyroxene associations; in rare occasions, orthopyroxene can be present.

The sanukitoid suite, as originally proposed by Shirey and Hanson (1984), Stern (1989), and Stern and Hanson (1991), represents a magmatic series which, at silica values of 60 wt.% or less, has MgO>6 wt.%, Mg#>0.60, Cr>100 ppm, Sr and Ba each >500 ppm, and high Na_2O, K_2O, LREE, and La/Yb. Closepet-type mainly differs from sanukitoid in having higher K_2O/Na_2O ratios, which can reach 1.0; it is also richer in Ti, Nb, and Zr. In contrast to TTG, sanukitoid and Closepet-type granite follow a classical calc–alkaline trend in the K–Na–Ca triangle (Fig. 7C). The high MgO, Mg#, Cr, Ni, and K_2O, in particular, clearly distinguish these magmas from TTGs of any age (Fig. 12).

4.2. Petrogenesis

The high Mg# (>>0.62) and high Cr and Ni concentrations in primitive members of the Archaean sanukitoid and Closepet-type suites preclude a crustal source, including basaltic crust. However, even the most primitive sanukitoids show extreme enrichments in LILE (Fig. 13) which, given the high Mg#, Cr, and Ni, cannot be the result of crystal fractionation.

In order to account for the genesis of these magmas, Stern (1989) modeled contamination of basaltic or komatiitic magmas by a LILE-rich felsic crust. They concluded that interaction between mafic or ultramafic melts and crustal material cannot produce both the high Ni and Cr, and the high SiO_2 and LILE compositions of primitive sanukitoids. A similar conclusion was reached by Smithies and Champion (1999a), although Stevenson et al. (1999) and Moyen et al. (1997) showed that crustal assimilation may become very important in the more felsic members of suites. Consequently, the most primitive compositions must derive from a peridotitic source but the composition of that mantle source must also be

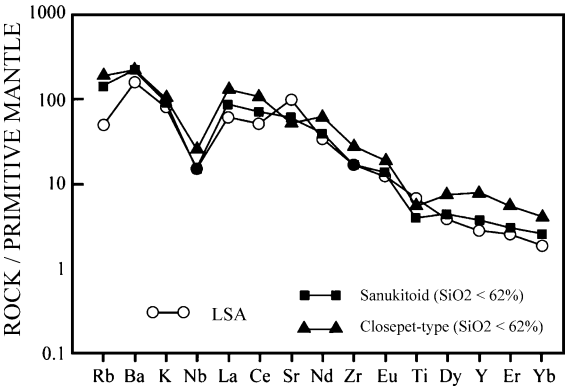

Fig. 13. Primitive mantle (McDonough et al., 1992) normalize multielement diagram for average LSA (○) compared with average sanukitoids (■) and average Closepet-type granite (▲) whose SiO_2 content is lower than 62%. Sanukitoids are very similar to LSA except for Sr and Rb contents. Average compositions are from Table 1.

able to account for the LILE-rich, HFSE-depleted nature of the rocks (e.g., Shirey and Hanson, 1984; Stern, 1989; Smithies and Champion, 1999b).

Despite contrasting with TTG in terms of Mg# and MgO, Cr, and Ni concentrations, Archaean sanukitoids also show many close similarities with both TTG and adakites. These similarities include high LILE and strongly fractionated REE patterns, with typically low Yb and Y concentrations (Fig. 13). In TTG and adakites, such features are interpreted to reflect a slab-melt signature. Consequently, re-melting of peridotite previously metasomatised via addition of slab-melt is regarded as the most likely petrogenetic model for Archaean sanukitoid (Shirey and Hanson, 1984; Stern, 1989; Stern and Hanson, 1991; Rapp et al., 1999; Smithies and Champion, 1999a).

4.3. Sanukitoids vs. HSA and LSA

Figs. 13 and 14 compare the less-differentiated ($SiO_2 \leq 62$ wt.%) sanukitoid and Closepet-type granite with LSA. For elements such as SiO_2, MgO, Sr, Cr, Ni, and Nb, LSA and sanukitoids have a very similar range that contrasts with the range for HSA. Fig. 13 also shows that the LSA trace element patterns also closely match those of sanukitoid, while Closepet-type granite shows a parallel pattern but at higher concentrations. However, it must be noted that LSA typically show significant positive Sr anomalies, which is not the case for sanukitoids. In addition, the low Rb content typical of LSA is not so pronounced in sanukitoids or Closepet-type granite. This is well exemplified in the K vs. Rb diagram (Fig. 14D) where data are widely scattered. Fig. 14E shows that LSA covers a wide range in TiO_2 content (0.5–3.5%). Because of the relative lack of Cr and Ni data for some sanukitoids, only few points were reported in the diagram; however, TiO_2 in sanukitoids ranges between 0.5 and 2.5, which is more similar with LSA.

The compositional similarities between sanukitoid and Closepet-type granite and LSA suggest a similar

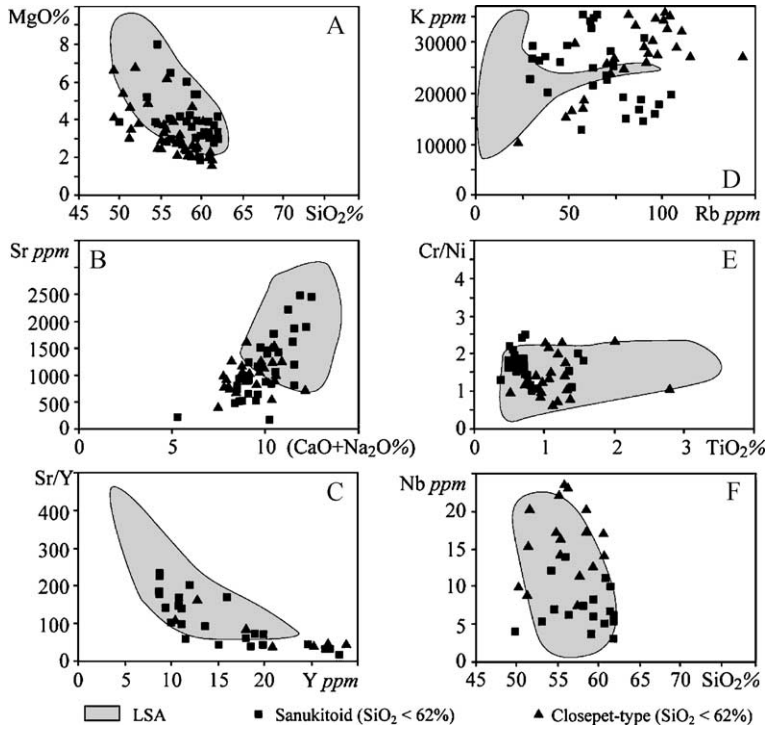

Fig. 14. MgO vs. SiO_2 (A); Sr vs. ($CaO+Na_2O$) (B); (Sr/Y) vs. Y (C); K vs. Rb (D); (Cr/Ni) vs. TiO_2 (E); and Nb vs. SiO_2 (F) diagrams comparing low-SiO_2 adakites (LSA; light grey field) with sanukitoids (■) and Closepet-type granites (▲) whose SiO_2 content is lower than 62%. Except for Rb and K_2O, there is a reasonable overlap between LSA, sanukitoids, and Closepet-type granites.

petrogenesis. The compositional differences pointed out above might result from two contrasting processes. Firstly, the sanukitoids and Closepet-type granites have all undergone more significant fractional crystallization. Secondly, as mentioned by Moyen et al. (2001) and Stevenson et al. (1999), many sanukitoid and Closepet-type magmas have been contaminated by continental crust, which has significantly altered LILE contents (such as K and Rb, e.g., Fig. 14D).

In summary, (1) sanukitoids and Closepet-type granite and LSA show several petrographic and chemical similarities; (2) the mechanisms invoked to account for their genesis are similar: i.e., melting of a mantle peridotite metasomatised by adakitic melts. Consequently, LSA can be considered as reasonable analogues for sanukitoids and Closepet-type primary magma genesis. The chemical differences between sanukitoids and Closepet-type magma could reflect differences in melting depth and/or be due to the subsequent evolution and differentiation, which produced compositions not typical of the LSA suite.

5. Comments and conclusion

The names ‘adakite’ and ‘TTG’ were originally defined to encompass rocks, or rock series, with specific compositional attributes thought to reflect a specific petrogenesis; melts derived from subducted basalt in the case of adakite, and melts of basaltic crust, in the case of TTG. Notably, even the original petrogenetic interpretations of these rocks emphasised commonalities (a basaltic source), of course reflected in close compositional overlap. It has now become apparent that, even within the original definitions, there is a range of compositions that reflect a range of possible petrogenetic models, although all with links to a basaltic source component.

The two main types of modern adakites can be defined on the basis of their silica content, amongst other compositional attributes. The contrasting distinction between high-SiO_2 adakite and low-SiO_2 adakite is not only a mineralogical or chemical compositional difference, but essentially emphasizes difference in source and petrogenesis. The primary source of HSA is subducted oceanic crust, but the resulting melts also interact with peridotite during their ascent through the mantle wedge. The source of LSA is a mantle peridotite whose composition has been modified (metasomatised) by adakitic melts.

Modern adakites appear mainly restricted to subduction settings that show unusually high heat-flow; e.g. during subduction of young oceanic crust, subduction initiation, ridge subduction, or flat subduction (i.e., Peacock, 1990, 1993; Gutscher et al., 2000a,b). Such situations are rare in modern subduction zones, thus accounting for the relative scarcity of modern adakites when compared with the abundance of classic calc-alkaline magmatism. In contrast, a similarly high heat flow is thought to have typified the Archaean Earth, where heat production was 3 to 4 times greater than today (Brown, 1985). This resulted in more efficient convection and in smaller plates (Hargraves, 1986; De Wit and Hart, 1993) leading to the subduction of younger and hotter oceanic plates. Hence, while the definition of TTG did not specify the environment of melting, it is now generally thought that it is also related to high-P melting of basalt in some form of subduction zone.

Both types of modern adakite have Archaean analogues. TTGs younger than ~3.3 Ga show virtually complete compositional overlap with high-SiO_2 adakite. Archaean sanukitoids and the compositionally similar Closepet-type granites have many close compositional similarities with low-SiO_2 adakites, and their petrogenesis is interpreted in the same way. Like the TTGs that resemble high-SiO_2 adakite, sanukitoids and Closepet-type granites so far appear restricted to the Late Archaean. From an uniformitarian perspective, such analogies indicate that modern-style subduction processes, including interaction between enriched slab-derived components and a mantle wedge, occurred as far back as ~3.3 Ga. Perhaps a more correct way to view this is that ancient styles of subduction that have operated since at least 3.3 Ga persist in a limited way today.

In contrast to Middle and Late Archaean TTGs, old TTGs differ from HSA in that they have systematically lower Mg#, Cr and Ni and higher SiO_2. The seemingly small compositional differences, however, reflect a rather fundamental petrogenetic shift from that of either type of adakite, Late Archaean TTG, and sanukitoid. For this reason, Smithies (2000) suggested that Early Archaean TTG was not analogous with adakite. As with HSA, all TTG are the products of basalt melting at high-pressure, and probably all also

result from some kind of subduction. The Early Archaean TTG differs from Late Archaean TTG and modern HSA in that the parental magmas underwent little or no interaction with mantle peridotite.

Because TTG form such a large proportion of Earth's juvenile continental crust, the small compositional differences between Early Archaean and Late Archaean TTG reflects a critical secular shift in the way continental crust formed. The changes can be directly related to the cooling of Earth. In the hotter pre-3.3 Ga part of the Archaean, two factors conspired to ensure that slab-melts seldom, if ever, interacted with mantle peridotite. Firstly, slab-melting occurred at a higher crustal level. Secondly, a thicker, more buoyant oceanic crust simply subducted at such a low angle that an effective mantle wedge never formed. The immediate implication is that mantle wedge sources played little or no role in the evolution of the crust before ~3.3 Ga.

The temporal evolution of slab-derived magmas can be tentatively summarized in the four following stages:

(1) In the Early Archaean (T>3.3 Ga), terrestrial heat production was important such that melting of subducted basalts occurred at shallow depth. In addition, the thicker oceanic crust was more buoyant and subduction was flat or at a very low angle. Consequently, there was no mantle wedge formation and TTG magmas had no possibility to interact with peridotite.
(2) In the Middle to Late Archaean, the heat production was lower and melting of the subducted slab occurred at greater depth. Similarly, the colder oceanic crust was thinner and less buoyant, such that subduction could occur at an angle (similar to modern subduction) that ensured the presence of a mantle wedge. The efficiency of slab-melting led to high slab-melt/mantle peridotite ratios. Thus, the slab melts were not totally consumed by reaction with mantle peridotite (Rapp et al., 1999), and so TTG magma were emplaced into the crust.
(3) During the Late Archaean, and particularly towards the Archaean–Proterozoic boundary, Earth heat production and the efficiency of slab melting had both declined. Slab-melt/mantle peridotite ratios had correspondingly declined such that some slab-melts were totally consumed in reaction with mantle peridotite (Rapp et al., 1999). Subsequent melting of this metasomatised mantle peridotite produced Archaean sanukitoids and Closepet-type granites.
(4) Since the Lower Proterozoic, Earth's heat production was too low to allow subducted slab-melting under 'normal' conditions. Consequently, a slab dehydrates and classic calc–alkaline magmatism results from melting of a peridotite that has been metasomatised by dehydration fluids. Now, LSA and HSA appear as exceptional remnants of an ancient style of subduction.

Acknowledgements

The authors are grateful to Bor Ming Jahn and John Tarney for their helpful comments and suggestions on the manuscript.

References

Abbott, D., Drury, R., Smith, W.H.F., 1994. Flat to steep transition in subduction style. Geology 22 (10), 937–940.

Adam, J., Green, T.H., Sie, S.H., 1993. Proton microprobe determined partitioning of Rb, Sr, Ba, Y, Zr, Nb and Ta between experimentally produced amphiboles and silicate melts with variable F content. Chem. Geol. 109, 29–49.

Arth, J.G., Hanson, G.N., 1975. Geochemistry and origin of the Early Precambrian crust of north-eastern Minnesota. Geochim. Cosmochim. Acta 39, 325–362.

Atherton, M.P., Petford, N., 1993. Generation of sodium-rich magmas from newly underplated basaltic crust. Nature 362, 144–146.

Balakrishnan, S., Rajamani, V., 1987. Geochemistry and petrogenesis of granitoids around Kolar schist belt: constraints for crustal evolution in Kolar area. J. Geol. 95, 219–240.

Barker, F., Arth, J.G., 1976. Generation of trondhjemitic–tonalitic liquids and Archaean bimodal trondhjemite–basalt suites. Geology 4, 596–600.

Barker, F., Arth, J.G., Millard, H.T., 1979. Archaean trondhjemites of the southwestern Big Horn Mountains, Wyoming: a preliminary report. In: Barker, F. (Ed.), Trondhjemites, Dacites and Related Rocks. Elsevier, Amsterdam, pp. 401–414.

Barton, J.M., Doig, R., Smith, C.B., Bohlender, F., van Reenen, D.D., 1992. Isotopic and REE characteristics of the intrusive charnoenderbite and enderbite geographically associated with

the Matok Pluton, Limpopo Belt, southern Africa. Precambrian Res. 55 (1–4), 451–467.

Beakhouse, G.P., Heaman, L.M., Creaser, R.A., 1999. Geochemical and U–Pb zircon geochronological constraints on the development of a Late Archean greenstone belt at Birch Lake, Superior Province, Canada. Precambrian Res. 97 (1–2), 77–97.

Beard, J.S., Lofgren, G.E., 1989. Effect of water on the composition of partial melts of greenstones and amphibolites. Science 144, 195–197.

Beard, J.S., Lofgren, G.E., 1991. Dehydration melting and water-saturated melting of basaltic and andesitic greenstones and amphibolites at 1, 3 and 6.9 kb. J. Petrol. 32, 465–501.

Bebout, G.E., Barton, M.D., 1993. Metasomatism during subduction: products and possible paths in the Catalina schist, California. Chem. Geol. 108, 61–92.

Bickle, M.J., 1986. Implications of melting for stabilisation of lithosphere and heat loss in the Archaean. Earth Planet. Sci. Lett. 80, 314–324.

Bourdon, E., Eissen, J.-P., Monzier, M., Robin, C., Martin, H., Joseph, C., Hall, M.L., 2002. Adakite-like lavas from Antisana Volcano (Ecuador): evidence for slab melt metasomatism beneath Andean northern volcanic zone. J. Petrol. 43 (2), 199–217.

Brown, G.C., 1985. Processes and problems in the continental lithosphère: geological history and physical implications. In: Snelling, N. (Ed.), Geochronology and Geological Record, Special Publication - Geological Society of London 10, pp. 326–334.

Calmus, T., Aguillon-Robles, A., Maury, R.C., Bellon, H., Benoit, M., Cotten, J., Bourgois, J., Michaud, F., 2003. Spatial and temporal evolution of basalts and magnesian andesites ("bajaites") from Baja California, Mexico: the role of slab melts. Lithos 66 (1–2), 77–105.

Champion, D.C., Sheraton, J.W., 1997. Geochemistry and Nd isotope systematics of Archaean granites of the Eastern Goldfields, Yilgarn Craton, Australia: implications for crustal growth processes. Precambrian Res. 83 (1–3), 109–132.

Champion, D.C., Smithies, R.H., 2003. Archaean granites. In: Blevin, P., Jones, M., Chappell, B. (Eds.), Magmas to Mineralisation: The Ishihara Symposium. Geoscience, Australia, pp. 19–24.

Champion, D.C., Smithies, R.H., 2003. Slab melts and related processes—Archaean versus Recent. In: Arima, M., Nakajima, T., Ishihara, S. (Eds.), Hutton Symposium V, The Origin of Granites and Related Rocks. Geological Survey of Japan, pp. 19.

Condie, K.C., 1981. Archaean Greenstone Belts. Elsevier, Amsterdam. 434 pp.

Condie, K.C., Swenson, D.H., 1973. Compositional variations in three Cascade stratovolcanoes: Jefferson, Rainier and Shasta. Bull. Volcanol. 37, 205–320.

Dalpé, C., Baker, D.R., 2000. Experimental investigation of large-ion-lithophile-element-, high-field-strength-element- and rare-earth-element-partitioning between calcic amphibole and basaltic melt: the effects of pressure and oxygen fugacity. Contrib. Mineral. Petrol. 140, 233–250.

Davies, G.F., 1992. On the emergence of plate tectonics. Geology 20 (11), 963–966.

de Wit, M.J., 1998. On Archean granites, greenstones, cratons and tectonics: does the evidence demand a verdict? Precambrian Res. 91 (1–2), 181–226.

de Wit, M.J., Hart, R.A., 1993. Earth's earliest continental lithosphere, hydrothermal flux and crustal recycling. Lithos 30, 309–335.

Defant, M.J., Drummond, M.S., 1990. Derivation of some modern arc magmas by melting of young subducted lithosphere. Nature 347, 662–665.

Defant, M.J., Clarck, L.F., Stewart, R.H., Drummond, M.S., de Boer, J.Z., Maury, R.C., Bellon, H., Jackson, T.E., Restrepo, J.F., 1991. Andesite and dacite genesis via contrasting processes: the geology and geochemistry of El Valle volcano, Panama. Contrib. Mineral. Petrol. 106, 309–324.

Defant, M.J., Jackson, T.E., Drummond, M.S., De Boer, J.Z., Bellon, H., Feigenson, M.D., Maury, R.C., Stewart, R.H., 1992. The geochemistry of young volcanism throughout western Panama and southeastern Costa Rica: an overview. J. Geol. Soc. (London) 149, 569–579.

Drummond, M.S., Defant, M.J., 1990. A model for trondhjemite–tonalite–dacite genesis and crustal growth via slab melting: Archaean to modern comparisons. J. Geophys. Res. 95, 21503–21521.

Evans, O.C., Hanson, G.N., 1997. Late- to post-kinematic Archean granitoids of the S.W. Superior Province: derivation through direct mantle melting. In: de Wit, M.J., Ashwal, L.D. (Eds.), Greenstone Belts. Oxford Univ. Press, Oxford, pp. 280–295.

Foley, S.F., Barth, M.G., Jenner, G.A., 2000. Rutile/melt partition coefficients for trace elements and an assessment of the influence of rutile on the trace element characteristics of subduction zone magmas. Geochim. Cosmochim. Acta 64, 933–938.

Foley, S.F., Tiepolo, M., Vannucci, R., 2002. Growth of early continental crust controlled by melting of amphibolite in subduction zones. Nature 417, 637–640.

Francis, D., Ludden, J., 1995. The signature of amphibole in mafic alkaline lavas, a study in the Northern Canadian Cordillera. J. Petrol. 36, 1171–1191.

Frost, C.D., Frost, B.R., Chamberlain, K.R., Hulsebosch, T.P., 1998. The late Archaean history of the Wyoming province as recorded by granitic magmatism in the Wind River Range. Wyoming. Precambrian Res. 89, 145–173.

Garrison, J.M., Davidson, J.P., 2003. Dubious case for slab melting in the northern volcanic zone of the Andes. Geology 31 (6), 565–568.

Gonzalez-Partida, E., Levresse, G., Carrillo-Chavez, A., Cheilletz, A., Gasquet, D., Jones, D., 2003. Paleocene adakite Au–Fe bearing rocks, Mezcala, Mexico: evidence from geochemical characteristics. J. Geochem. Explor. 80, 25–40.

Green, T.H., Pearson, N.J., 1987. An experimental study of Nb and Ta partitioning between Ti-rich minerals and silicate liquids at high pressure and temperature. Geochim. Cosmochim. Acta 51, 55–62.

Gutscher, M.-A., Maury, F., Eissen, J.-P., Bourdon, E., 2000. Can slab melting be caused by flat subduction? Geology 28 (6), 535–538.

Gutscher, M.-A., Spakman, W., Bijwaard, H., Engdahl, E.R., 2000. Geodynamics of flat subduction: seismicity and tomographic constraints from the Andean margin. Tectonics 19 (5), 814–833.

Hargraves, R.B., 1986. Faster spreading or greater ridge length in the Archaean. Geology 14, 750–752.

Helz, R.T., 1976. Phase relations in basalts in their melting range at $P(H_2O)$=5 kb. Part II: melt compositions. J. Petrol. 17, 139–193.

Holloway, J.R., Burnham, C.W., 1972. Melting relations of basalt with equilibrium water pressure less than total pressure. J. Petrol. 13, 1–29.

Hunter, D.R., Barker, F., Millard, H.T., 1978. The geochemical nature of the Archaean ancient gneiss complex and granodioritic suite, Swaziland: a preliminary study. Precambrian Res. 7, 105–127.

Ionov, D.A., Hofmann, A.W., 1995. Nb–Ta-rich mantle amphiboles and micas: implications for subduction-related metasomatic trace element fractionations. Earth Planet. Sci. Lett. 131 (3–4), 341–356.

Jahn, B.M., Glikson, A.Y., Peucat, J.-J., Hickman, A.H., 1981. REE geochemistry and isotopic data of Archaean silicic volcanics and granitoids from the Pilbara Block, western Australia: implications for the early crustal evolution. Geochim. Cosmochim. Acta 45, 1633–1652.

Jahn, B.M., Auvray, B., Shen, Q.H., Liu, D.Y., Zhang, Z.Q., Dong, Y.J., Ye, X.J., Zhang, Q.Z., Cornichet, J., Macé, J., 1988. Archaean crustal evolution in China: the Taishan complex, and evidence for juvenile crustal addition from long-term depleted mantle. Precambrian Res. 38, 381–403.

Jayananda, M., Martin, H., Peucat, J.-J., Mahabaleswar, B., 1995. Late Archaean crust–mantle interactions in the Closepet granite, Southern India: evidence from Sr–Nd isotopes, major and trace element geochemistry. Contrib. Mineral. Petrol. 119, 314–329.

Kay, R.W., 1978. Aleutian magnesian andesites: melts from subducted Pacific Ocean crust. J. Volcanol. Geotherm. Res. 4, 117–132.

Kelemen, P.B., Johnson, K.T.M., Kinzler, R.J., Irving, A.J., 1990. High-field-strength element depletion in arc basalts due to mantle–magma interaction. Nature 345, 521–524.

Kepezhinskas, P.K., Defant, M.J., Drummond, M.S., 1995. Na metasomatism in the island arc mantle by slab melt–peridotite interaction: evidence from mantle xenoliths in the north Kamchatka arc. J. Petrol. 36, 1505–1527.

Kepezhinskas, P.K., Defant, M.J., Drummond, M.S., 1996. Progressive enrichment of island arc mantle by melt–peridotite interaction inferred from Kamchatka xenoliths. Geochim. Cosmochim. Acta 60, 1217–1229.

Klein, M., Stosch, H.-G., Seck, H.A., 1997. Partitioning of high field-strength and rare-earth elements between amphibole and quartz-dioritic to tonalitic melts: an experimental study. Chem. Geol. 138, 257–271.

Krogstad, E.J., Hanson, G.N., Rajamani, V., 1995. Sources of continental magmatism adjascent tolate Archaean Kolar suture zone, south India: distinct isotopic and elemental signatures of two late Archaean magmatic series. Contrib. Mineral. Petrol. 122, 159–173.

Lemarchand, F., Villemant, B., Calas, G., 1987. Trace element distribution coefficients in alkaline series. Geochim. Cosmochim. Acta 51, 1071–1081.

Lobach-Zhuchenko, S.B., Chekulaev, V.P., Ivanikov, V.V., Kovalenko, A.V., Bogomolov, E.S., 2000. Late Archaean high-Mg and subalkaline granitoids and lamprophyres as indicators of gold mineralization in Karelia (Baltic shield) Russia. In: Kremenetsky, A.A., Lehman, B., Seltmann, R. (Eds.), Ore-Bearing Granites of Russia and Adjacent Countries. INTAS, Moscow, pp. 193–211.

Lobach-Zhuchenko, S.B., Kovalenko, A.V., Krylov, I.N., Levskii, L.K., Bogomolov, E.S., 2000. Geochemistry and petrology of the ancient Vygozero granitoids, Southern Karelia. Geochem. Int. 38, 584–599.

Lobach-Zhuchenko, S.B., Rollinson, H., Chekulaev, V.P., Arestova, N.A., Kovalenko, A.V., Ivanikov, V.V., Guseva, N.S., Sergeev, S.A., Matukov, D.I., Jarvis, K.E., 2005. The Archaean sanukitoid series of the Baltic shield—geological setting, geochemical characteristics and implications for their origin. Lithos. 79, 107–128 (this issue).

Lopez-Escobar, L., Frey, F.A., Vergara, M., 1977. Andesites and high-alumina basalts from Central South Chile high Andes: geochemical evidences bearing to their petrogenesis. Contrib. Mineral. Petrol. 63, 199–228.

Mahlburg Kay, S., Ramos, V.A., Marquez, M., 1993. Evidence in Cerro Pampa volcanic rocks of slab melting prior to ridge trench collision in southern South America. J. Geol. 101, 703–714.

Martin, H., 1986. Effect of steeper Archean geothermal gradient on geochemistry of subduction-zone magmas. Geology 14, 753–756.

Martin, H., 1987. Petrogenesis of Archaean trondhjemites, tonalites and granodiorites from eastern Finland: major and trace element geochemistry. J. Petrol. 28 (5), 921–953.

Martin, H., 1988. Archaean and modern granitoids as indicators of changes in geodynamic processes. Rev. Bras. Geocienc. 17, 360–365.

Martin, H., 1994. The Archean grey gneisses and the genesis of the continental crust. In: Condie, K.C. (Ed.), The Archean Crustal Evolution, Developments in Precambrian Geology. Elsevier, Amsterdam, pp. 205–259.

Martin, H., 1999. The adakitic magmas: modern analogues of Archaean granitoids. Lithos 46 (3), 411–429.

Martin, H., Moyen, J.-F., 2002. Secular changes in TTG composition as markers of the progressive cooling of the Earth. Geology 30 (4), 319–322.

Martin, H., Moyen, J.-F., 2003. Secular changes in TTG composition: comparison with modern adakites. EGS-AGU-EUG joint meeting, Nice, April, VGP7-1FR2O-001.

Martin, H., Chauvel, C., Jahn, B.M., 1983. Major and trace element geochemistry and crustal evolution of granodioritic Archaean rocks from eastern Finland. Precambrian Res. 21, 159–180.

Maury, R.C., Sajona, F.G., Pubellier, M., Bellon, H., Defant, M.J., 1996. Fusion de la croûte océanique dans les zones de subduction/collision récentes: l'exemple de Mindanao (Philippines). Bull. Soc. Geol. Fr. 167 (5), 579–595.

McDonough, W.F., Sun, S.-S., 1995. Composition of the Earth. Chem. Geol. 120, 223–253.

McDonough, W.F., Sun, S.-S., Ringwood, A.E., Jagoutz, E., Hofmann, A.W., 1992. Potassium, rubidium, and cesium in the

Earth and Moon and the evolution of the mantle of the Earth. Geochim. Cosmochim. Acta 56 (3), 1001–1012.

Morris, P.A., 1995. Slab melting as an explanation of Quaternary volcanism and aseismicity in southwestern Japan. Geology 23, 395–398.

Moyen, J.-F., Martin, H., Jayananda, M., 1997. Origine du granite fini-Archéen de Closepet (Inde du Sud): apports de la modélisation géochimique du comportement des éléments en traces. C. R. Acad. Sci. Paris 325, 659–664.

Moyen, J.-F., Martin, H., Jayananda, M., 2001. Multi-element geochemical modelling of crust–mantle interactions during late-Archaean crustal growth: the Closepet granite (South India). Precambrian Res. 112, 87–105.

Moyen, J.-F., Martin, H., Jayananda, M., Auvray, B., 2003. Late Archaean granites: a typology based on the Dharwar Craton (India). Precambrian Res. 127 (1–3), 103–123.

Moyen, J.-F., Nedelec, A., Martin, H., Jayananda, M., 2003. Syntectonic granite emplacement at different structural levels: the Closepet granite, South India. J. Struct. Geol. 25 (4), 611–631.

Peacock, S.M., 1990. Fluid processes in subduction zones. Science 248, 329–337.

Peacock, S.M., 1993. Large-scale hydration of the lithosphere above subducting slabs. Chem. Geol. 108, 43–59.

Peacock, S.M., Rushmer, T., Thompson, A.B., 1994. Partial melting of subducting oceanic crust. Earth Planet. Sci. Lett. 121, 224–227.

Pearce, J.A., Norry, M.J., 1979. Petrogenetic implications of Ti, Zr, Y and Nb variations in the volcanic rocks. Contrib. Mineral. Petrol. 69, 33–47.

Petford, N., Gallagher, K., 2001. Partial melting of mafic (amphibolitic) lower crust by periodic influx of basaltic magma. Earth Planet. Sci. Lett. 193 (3–4), 483–499.

Prouteau, G., Maury, R.C., Rangin, C., Suparka, E., Bellon, H., Pubellier, M., Cotten, J., 1996. Les adakites miocènes du NW de Bornéo, témoins de la fermeture de la proto-mer de Chine. C. R. Acad. Sci. Paris 323, 925–932.

Prouteau, G., Scaillet, B., Pichavant, M., Maury, R.C., 2001. Evidence for mantle metasomatism by hydrous silicic melts derived from subducted oceanic crust. Nature 410, 197–200.

Querré, G., 1985. Palingenèse de la croûte continentale à l'Archéen: les granitoïdes tardifs (2,5–2,4 Ga.) de Finlande orientale; pétrologie et géochimie, Mém. Docum. Centre Arm. Docum. Centre Arm. Et Struct. Socles. Université de Rennes, Rennes, pp. 226.

Rapp, R.P., 2003. Experimental constraints on the origin of compositional variations in the adakite-TTG-sanukitoid-HMA family of granitoids EGS-AGU-EUG joint meeting, Nice, April, VGP7-1FR2O-005.

Rapp, R.P., Watson, E.B., 1995. Dehydration melting of metabasalt at 8–32 kbar: implications for continental growth and crust–mantle recycling. J. Petrol. 36 (4), 891–931.

Rapp, R.P., Watson, E.B., Miller, C.F., 1991. Partial melting of amphibolite/eclogite and the origin of Archaean trondhjemites and tonalites. Precambrian Res. 51, 1–25.

Rapp, R.P., Shimizu, N., Norman, M.D., Applegate, G.S., 1999. Reaction between slab-derived melts and peridotite in the mantle wedge: experimental constraints at 3.8 GPa. Chem. Geol. 160, 335–356.

Rapp, R.P., Shimizu, N., Norman, M.D., 2003. Growth of early continental crust by partial melting of eclogite. Nature 425, 605–609.

Regan, M.K., Gill, J.B., 1989. Coexisting calc–alkaline and high-niobium basalts from Turrialba volcano, Costa Rica: implications for residual titanates in arc magma sources. J. Geophys. Res. 94, 4619–4633.

Rogers, G., Saunders, A.D., Terrell, D.J., Verma, S.P., Marriner, G.F., 1985. Geochemistry of Holocene volcanic rocks associated with ridge subduction in Baja California, Mexico. Nature 315, 389–392.

Rollinson, H., 1993. Using Geochemical Data: Evaluation, Presentation, Interpretation. Longman, London. 352 pp.

Rushmer, T., 1991. Partial melting of two amphibolites: contrasting experimental results under fluid-absent conditions. Contrib. Mineral. Petrol. 107, 41–59.

Sajona, F.G., 1995. Fusion de la croûte océanique en contexte de subduction collision: géochimie, géochronologie et pétrologie du magmatisme plioquaternaire de Mindanao (Philippines) Université Thesis, Bretagne Occidentale, Brest, 223 pp.

Sajona, F.G., Bellon, H., Maury, R., Pubellier, M., Quebral, R., Cotten, J., Bayon, F., Pagado, E., Pamatian, P., 1997. Tertiary and Quaternary magmatism in Mindanao and Leyte (Philippines); geochronology, geochemistry and tectonic setting. J. Asian Earth Sci. 15 (2–3), 121–153.

Sajona, F.G., Maury, R., Bellon, H., Cotten, J., Defant, M.J., 1996. High field strength element enrichment of Pliocene–Pleistocene island arc basalts, Zamboanga Peninsula, western Mindanao (Philippines). J. Petrol. 37 (3), 693–726.

Samaniego, P., Martin, H., Robin, C., Monzier, M., 2002. Transition from calc–alkalic to adakitic magmatism at Cayambe volcano, Ecuador: insights into slab melts and mantle wedge interactions. Geology 30 (11), 967–970.

Samaniego, P., Martin, H., Robin, C., Monzier, M., Cotten, J., 2004. Temporal evolution of magmatism at Northern Vocanic Zone of the Andes: the geology and petrology of Cayambe volcanic complex (Ecuador). J. Petrol. (in press).

Samsonov, A.V., Bogina, M.M., Bibikova, E.V., Petrova, A.Y., Shchipansky, A.A., 2005. The relationship between adakitic, calc–alkaline volcanic rocks and TTGs: Implications for tectonic setting of the Karelian greenstone belts, Baltic Shield. Lithos. 79, 83–106 (this issue).

Sarvothaman, H., 2001. Archaean high-Mg granitoids of mantle origin in the Eastern Dharwar Craton of Andhra Pradesh. J. Geol. Soc. India 58, 261–268.

Schiano, P., Clochiatti, R., Shimizu, N., Maury, R.C., Jochum, K.P., Hofman, A.W., 1995. Hydrous, silica-rich melts in the sub-arc mantle and their relationships with erupted arc lavas. Nature 377, 595–600.

Schmidt, M.W., Poli, S., 1998. Experimentally based water budgets for dehydrating slabs and consequences for arc magma generation. Earth Planet. Sci. Lett. 163 (1–4), 361–379.

Sen, C., Dunn, T., 1994. Dehydration melting of a basaltic composition amphibolite at 1.5 and 2.0 Gpa: implications

for the origin of adakites. Contrib. Mineral. Petrol. 117, 394–409.
Sen, C., Dunn, T., 1994. Experimental modal metasomatism of a spinel lherzolite and the production of amphibole-bearing peridotite. Contrib. Mineral. Petrol. 119, 422–432.
Sheraton, J.W., Black, L.P., 1983. Geochemistry of Precambrian gneisses: relevance for the evolution of the east Antarctic shield. Lithos 16, 273–296.
Shirey, S.B., Hanson, G.N., 1984. Mantle derived Archaean monzodiorites and trachyandesites. Nature 310, 222–224.
Shirey, S.B., Hanson, G.N., 1986. Mantle heterogeneity and crustal recycling in Archaean granite–greenstone belts: evidence from Nd isotopes and trace elements in the Rainy Lake province, Ontario, Canada. Geochim. Cosmochim. Acta 50, 2631–2651.
Sigmarsson, O., Martin, H., Knowles, J., 1998. Melting of a subducting oceanic crust from U–Th disequilibria in Austral Andean lavas. Nature 394, 566–569.
Smith, D.R., Leeman, W.P., 1987. Petrogenesis of the Mt. St. Helens dacitic magmas. J. Geophys. Res. 92, 10313–10334.
Smithies, R.H., 2000. The Archaean tonalite–trondhjemite–granodiorite (TTG) series is not an analogue of Cenozoic adakite. Earth Planet. Sci. Lett. 182, 115–125.
Smithies, R.H., Champion, D.C., 1999. High-Mg diorite from the Archaean Pilbara Craton: anorogenic magmas derived from a subduction-modified mantle. Geol. Surv. West. Aust. Annu. Rev. 1998–1999, 45–59.
Smithies, R.H., Champion, D.C., 1999. Late Archaean felsic alkaline igneous rocks in the Eastern Goldfields, Yilgarn Craton, Western Australia: a result of lower crustal delamination? J. Geol. Soc. (London) 156 (3), 561–576.
Smithies, R.H., Champion, D.C., 2000. The Archaean high-Mg diorite suite: links to tonalite–trondhjemite–granodiorite magmatism and implications for early Archaean crustal growth. J. Petrol. 41 (12), 1653–1671.
Smithies, R.H., Champion, D.C., 2001. Archaean granites of the Ylgarn and Pilbara cratons, Western Australia. AGSO Geosci. Aust., 134–136.
Smithies, R.H., Champion, D.C., Cassidy, K.F., 2003. Formation of Earth's early Archaean continental crust. Precambrian Res. 127 (1–3), 89–101.
Sorensen, S.S., 1988. Petrology of amphibolite–facies mafic and ultramafic rocks from Catalina schist, southern California: metamorphism and migmatisation in a subduction zone metamorphic setting. J. Metamoprh. Geol. 6, 405–435.
Sorensen, S.S., Barton, M.D., 1987. Metasomatism and partial melting in a subduction complex: Catalina schist, southern California. Geology 15, 115–118.
Sorensen, S.S., Grossman, J.N., 1989. Enrichment in trace elements in garnet amphibolites from a paleo-subduction zone: Catalina schist, southern California. Geochim. Cosmochim. Acta 53, 3155–3177.
Stern, R., 1989. Petrogenesis of the Archaean Sanukitoid Suite. State University at Stony Brook, New York. 275 pp.
Stern, C.R., Futa, K., 1982. An Andean andesite derived directly from subducted MORB or from LIL depleted subcontinental mantle. Trans. - Am. Geophys. Union 63, 1148.
Stern, R.A., Hanson, G.N., 1991. Archaean high-Mg granodiorite: a derivative of light rare earth enriched monzodiorite of mantle origin. J. Petrol. 32, 201–238.
Stern, C.R., Kilian, R., 1996. Rôle of the subducted slab, mantle wedge and continental crust in the generation of adakites from the Austral Volcanic Zone. Contrib. Mineral. Petrol. 123, 263–281.
Stevenson, R., Henry, P., Gariépy, C., 1999. Assimilation–fractional crystallization origin of Archaean sanukitoid suites: Western Superior Province, Canada. Precambrian Res. 96, 83–99.
Sylvester, P.J., 1994. Archaean granite plutons. In: Condie, K.C. (Ed.), The Archean Crustal Evolution, Developments in Precambrian Geology. Elsevier, Amsterdam, pp. 261–314.
Tarney, J., Jones, C.E., 1994. Trace element geochemistry of orogenic rocks and crustal growth models. J. Geol. Soc. (London) 151, 855–868.
Tarney, J., Weaver, B.L., Drury, S.A., 1979. Geochemistry of Archaean trondhjemitic and tonalitic gneisses from Scotland and E. Greenland. In: Barker, F. (Ed.), Trondhjemites, Dacites and Related Rocks. Elsevier, Amsterdam, pp. 275–299.
Tarney, J., Weaver, B.L., Winley, B.F., 1982. Geological and geochemical evolution of the Archaean continental crust. Rev. Bras. Geocienc. 12, 53–59.
Tatsumi, Y., Ishizaka, K., 1982. Origin of high-magnesian andesites in the Setouchi volcanic belt, southwest Japan: I. Petrographical and chemical characteristics. Earth Planet. Sci. Lett. 60 (2), 293–304.
Tatsumi, Y., Nakamura, N., 1986. Composition of aquaeous fluid from serpentinite in the subducted lithosphere. Geochim. J. 20, 191–196.
Tatsumi, Y., Hamilton, D.L., Nesbitt, R.W., 1986. Chemical characteristics of fluid phase from the subducted lithosphere: evidence from high-pressure experiments and natural rocks. J. Volcanol. Geotherm. Res. 29, 293–309.
Taylor, S.R., McLennan, S.M., 1985. The Continental Crust: Its Composition and Evolution. Blackwell Scientific Publications, Oxford. 312 pp.
Thorpe, R.S., Francis, P.W., O'Callaghan, L., 1984. Relative roles of source composition, fractional crystallization and crustal contamination in the petrogenesis of Andean volcanic rocks. Philos. Trans. R. Soc. Lond., A 310, 675–692.
Wilson, M., 1991. Igneous Petrogenesis: A Global Tectonic Approach. Harper Collins Academic. 466 pp.
Winther, T.K., Newton, R.C., 1991. Experimental melting of an hydrous low-K tholeiite: evidence on the origin of Archaean cratons. Bull. Geol. Soc. Den., 39.
Wolf, M.B., Wyllie, P.J., 1991. Dehydration-melting of solid amphibolite at 10 kbar: textural development, liquid interconnectivity and applications to the segregation of magmas. Contrib. Mineral. Petrol. 44, 151–179.
Wolf, M.B., Wyllie, P.J., 1994. Dehydration-melting of amphibolite at 10 kbar: the effects of temperature and time. Contrib. Mineral. Petrol. 115, 369–383.
Xu, J.-F., Shinjo, R., Defant, M.J., Wang, Q., Rapp, R.P., 2002. Origin of Mesozoic adakitic intrusive rocks in the Ningzhen

area of east China: partial melting of delaminated lower continental crust? Geology 30 (12), 1111–1114.

Yogodzinski, G.M., Kay, R.W., Volynets, O.N., Koloskov, A.V., Kay, S.M., 1995. Magnesian andesite in the western Aleutian Komandorsky region: implications for slab melting and processes in the mantle wedge. Geol. Soc. Am. Bull. 107 (5), 505–519.

Zamora, D., 2000. Fusion de la croûte océanique subductée: approche expérimentale et géochimique. Université Thesis Université Blaise Pascal, Clermont-Ferrand, 314 pp.